CHALMERS
UNIVERSITY OF TECHNOLOGY

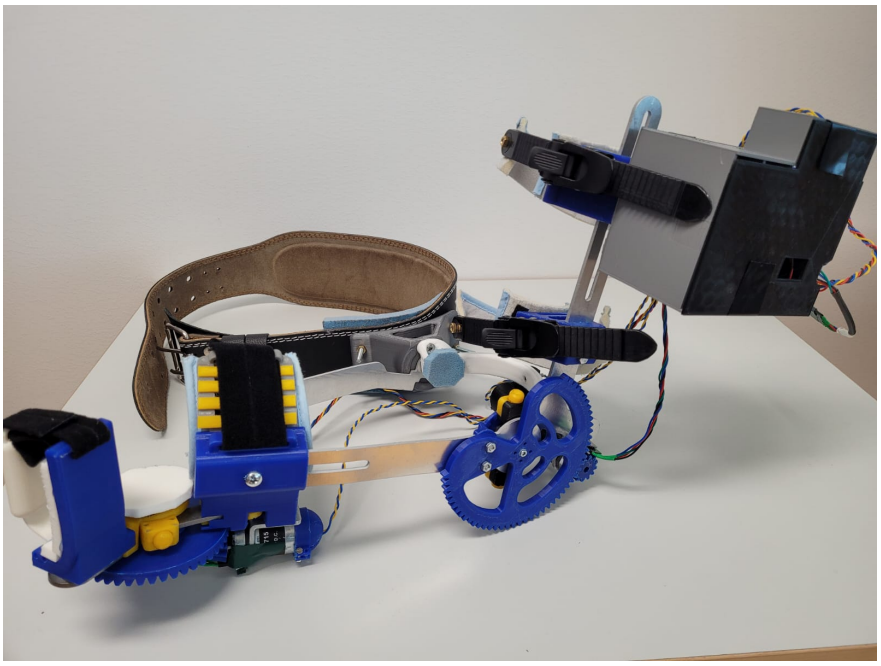

Iteration on a Stroke Rehabilitation Orthosis

Using Gravity Compensation and Assist-As-Needed Functionality

Master's Thesis in Biomedical Engineering

Christoffer Warefelt & Kyle Hollis

DEPARTMENT OF ELECTRICAL ENGINEERING

CHALMERS UNIVERSITY OF TECHNOLOGY
Gothenburg, Sweden 2023
www.chalmers.se

Master's thesis 2023

Iteration on a Stroke Rehabilitation Orthosis

Using Gravity Compensation and Assist-As-Needed Functionality

Christoffer Warefelt & Kyle Hollis

CHALMERS
UNIVERSITY OF TECHNOLOGY

Department of Electrical Engineering
Division of Biomedical Engineering
Center for Bionics and Pain Research
Chalmers University of Technology
Gothenburg, Sweden 2023

Iteration on a Stroke Rehabilitation Orthosis
Using Gravity Compensation and Assist-As-Needed Functionality
Christoffer Warefelt & Kyle Hollis

Supervisor: Morten B. Kristoffersen, Center for Bionics and Pain Research
Examiner: Max Ortiz Catalan, Center for Bionics and Pain Research

Master's Thesis 2023
Department of Electrical Engineering
Division of Biomedical Engineering
Center for Bionics and Pain Research
Chalmers University of Technology
Gothenburg

Cover: The state of the stroke rehabilitation orthosis prototype at the completion of this project.

Iteration on a Stroke Rehabilitation Orthosis
Using Gravity Compensation and Assist-As-Needed Functionality
Christoffer Warefelt & Kyle Hollis
Department of Electrical Engineering
Chalmers University of Technology

Abstract

One line of research at the Center for Bionics and Pain Research (CBPR) has been to develop an arm orthosis to aid in the rehabilitation of stroke patients with chronic symptoms. The end goal is a device that employs gravity compensation and assist-as-needed functionality on rehab exercise movements and can go home with the patient and integrate with CBPR's existing BioPatRec platform for EMG-based control and serious gaming. The previous iteration of the orthosis resulted in a mechanical device that could support and actuate the arm in one degree of freedom but had several shortcomings. The implementation of the servo motor limited the ability to perform gravity compensation or assist-as-needed control, as well as preventing the EMG classifier from transferring poorly to actual use since it cannot be worn during the training of the classifier.

Through the course of this project, the orthosis was iterated upon to bring it closer to the end goal of a functioning take-home stroke rehabilitation solution. The servo motor was replaced with a brushed DC motor, which both allowed for the development of a controller capable of gravity compensation and assist-as-needed control, and allowed for a passively backdrivable drive train that lets the system be worn during EMG classifier training. Additionally, the GUI was rebuilt to manage the increased functionality, the were improvements to the overall mechanical design, and a drive-train to the wrist joint was implemented. The latter opened up the possibility of including wrist rehabilitation, which should improve the quality of life for the patient. These changes moved the orthosis closer to becoming a functional rehabilitation device. They were evaluated in a small preliminary trial. The results of the preliminary trial look optimistic, however there are a number of ways the orthosis must be improved before it is ready for patient testing.

Acknowledgements

We would like to show gratitude to our supervisor Morten, for his feedback and encouragement throughout the entire project. Furthermore, a big thank you to all the colleagues at CBPR who helped both during testing but also brightened the days with various interactions. We would also like to thank our opponents for their feedback on our project. Our gratitude also goes out to the people at T-RAX who helped us with cutting the metal parts used in the orthosis. Lastly, we want to thank Max for being the examiner and enabling us to work on this project.

Christoffer Warefelt & Kyle Hollis, Gothenburg, June 21, 2023

Contents

List of Figures

1
Introduction

Stroke is one of the leading causes of disability in adults, and up to 70% of stroke survivors experience upper limb impairments [1]. To regain upper limb function, intense rehabilitation is needed, but unfortunately, most stroke survivors do not receive sufficient rehabilitation, partly due to insufficient resources in the healthcare system [2]. A solution to this is one of the ongoing directions of research at the Center for Bionics and Pain Research (CBPR), which is a collaboration between Chalmers Technical University, Gothenburg University, and Sahlgrenska University Hospital. CBPR has two separate platforms for reading and processing Electromyography (EMG) signals [3]. The first, BioPatRec, is currently used for research, while the second, MyoCognition, is still in development. Both platforms use EMG signals to control orthoses and prosthetics for rehabilitation using virtual limbs and serious games, a research direction being explored in the context of stroke.

1.1 Stroke Rehabilitation Today

Strokes occur when the blood flow to the brain is disrupted, either by obstruction or rupture [4]. Unless the interruption is resolved quickly, the affected part of the brain is deprived of the necessary oxygen and nutrients, and the brain cells die. The precise effects and severity depend on which part(s) of the brain become damaged. Still, the most common symptoms are paralysis on the opposite side of the body, speech/language or vision problems, behavioral changes, and memory loss.

Temporary or chronic paralysis or hemiparesis can significantly detract from the quality of life. To recover, the body enters a period of increased neuroplasticity similar to early brain development allowing the stroke patient to retrain motor programs along new neural pathways [5]. While this plastic process lasts roughly three months, the ability to train neural pathways and resolve stroke-related impairment never really ends [6]. The path to healing said impairment during the early stages of stroke recovery and beyond has been categorized into seven stages by the Brunnstrom model [7]:

1. Flaccidity
2. Spasticity appears
3. Increased spasticity
4. Decreased spasticity
5. Complex movement returns

6. Spasticity disappears
7. Normal function returns

The path from paralysis to recovery is not always straightforward. Stroke survivors can find themselves at any point along this path, from paralysis to spasticity to functionality. The different stages can take widely different amounts of time to move through, and the rehabilitation techniques and their goals are not the same for every stage [8]. Many stroke patients never fully recover, and experience chronic symptoms years or even decades later. Nevertheless, continued rehabilitation practice to progress through the stages is pivotal for retraining normal bodily function and minimizing affected limbs adapting to non-use.

1.2 Strokes and Muscle Activation

To perform the many complex body movement tasks that one learns to execute throughout their life, the brain creates task-specific motor programs that synergize the necessary muscles [5]. These synergies lie on a spectrum of specificity, as some motor programs require very specific muscles while others can broadly apply to various muscle groups depending on context. These synergies are thought to be stored anatomically as synergy-specific interneuron networks along the corticospinal tract, arranged with the most general synergies closer to the motor cortex and the more specific synergies further downstream along the motor pathway. This allows the brain to store a command as low-dimensional information, such as lifting an object off a table, that gets progressively refined into high-dimensional information, such as innervating specific muscles at specific times to specific degrees, as the command travels down the motor pathway.

When a stroke causes hemiparesis, it disrupts this motor pathway and fundamentally alters the synergies at the point of the lesion. The ability of the motor pathway to translate motor programs from the brain into muscle-specific signals is disrupted. This causes the command from the motor cortex to not result in the correct muscular activation. This can cause various symptoms depending on the severity of the stroke, which results in partial, incorrect, or even no muscle activation.

1.3 Abnormal Synergistic Movements

The first stage of the Brunnstrom model, flaccidity, is the period in which the brain cannot innervate the affected muscles at all [7]. The neuromuscular connection eventually reestablishes, but the synergies along the motor pathway need to be retrained [5]. The body attempts to accommodate for this debilitation by upregulating the surrounding motor pathways to take advantage of redundancy in the motor-neural activation path. Between the unexpected new usage of these surrounding motor pathways and the increased neural plasticity, while training new synergies, it is common for stroke patients to develop abnormal synergies that cause

unwanted groupings of muscle movements when they attempt to use the affected limb. Even the constant need to activate the muscles to carry the limb's weight against gravity can activate these maladapted synergies when using the arm [9].

Understanding these abnormal synergistic movements and training them into new well-adapted synergies is a primary goal of the rehabilitation process [7]. In stroke rehabilitation, the term 'synergistic movements' is often used to refer to the unintentional movements caused by these maladapted synergies. Upper limb synergistic movements can be categorized into flexor and extensor synergies. In the upper limbs, this is seen by all the joints – finger, wrist, elbow, and shoulder – being activated together either in flexion or extension, as seen in Figure 1.1. Synergistic movements are present in stages two through five of the Brunnstrom model, and rehabilitation exercises during these stages mainly focus on training away synergistic movements through repeated isolated exercises.

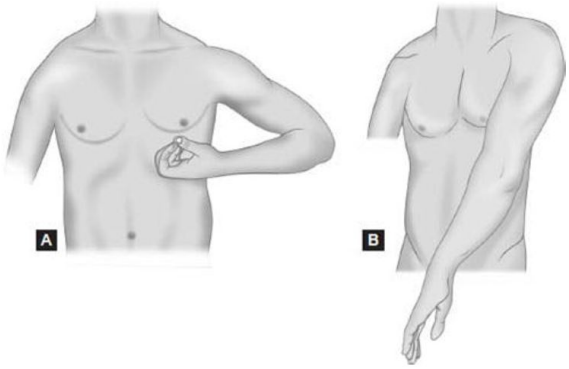

Figure 1.1: Upper limb maladapted synergistic movements during stroke rehabilitation express as flexion (A) and extension (B). Image used under fair use for educational purposes only [7].

1.4 Types of Stroke Rehabilitation

There are several ways to go about stroke rehabilitation. The patient can perform some tests to evaluate the degree of motor function and range of motion [10, 11]. Generally, stroke rehabilitation is repetitive and time-consuming, leading to novel approaches to make rehabilitation more exciting and feel like less of a chore for the patient [12]. Task-specific exercises have been shown to facilitate cortical plasticity in the brain and play a vital role in motor recovery [2, 13]. Due to the monotonous nature of the exercises, there are several novel approaches to making them more engaging and less resource-intensive [14]. One such approach is using an orthosis to enable the patient to perform the movements, by aiding the movement based on their surface Electromyography (sEMG or, henceforth, just EMG) signals. EMG is widely used in medical applications to study muscle movements [15]. These EMG signals can also be read and interpreted to, for example, control a character in a video game. Furthermore, EMG offers a low-power non-invasive method of measuring muscle innervation that can be adapted for orthoses.

1.5 EMG in Controlling Orthoses and Prostheses

EMG offers exciting possibilities for developing intelligent stroke rehabilitation devices by using the user's myoelectric signals to control the device. This application is explored largely in the context of active prostheses [16, 17, 18], but has also percolated into the scope of orthoses [19, 20, 2]. A large stumbling block in seeing this technology reach a functional level is the challenge of decoding muscle volition from the myoelectric signals [18]. Many traditional methods of decoding muscle volition struggle to achieve robust control over multiple degrees of freedom (DOF) [16]. The growing field of machine learning offers a solution, as intelligent learning networks performing EMG pattern recognition have shown success for multiple-DOF control. Deep learning networks have shown a high degree of precision when classifying multiple-DOF myoelectric signals when in testing environments but are struggling to translate into usable medical devices [18].

Several challenges must be overcome before this technology can mature into a usable state [16]. The variability in muscle contraction force and limb position for the same class of movement is much greater during daily-life use than in a controlled test environment, which greatly increases the complexity of the classification task and creates difficulty in collecting relevant training data for the network. EMG signal acquisition usually requires a matrix of electrodes and is susceptible to disturbances from the environment or misuse [21]. Creating an acquisition system for personal home use is often a choice between resolution, cost, and comfort. The repeatability of measurements is also a consideration, as a take-home system must be reliably used by untrained personnel. Wearable electronics, where the sensors are embedded in a piece of clothing, offer a reasonable compromise between these factors. Recent innovations have allowed the processing power and energy requirements for interpreting meaningful data from a matrix of sensors to become sufficiently small and affordable to be used in wearable devices [15].

Additionally, EMG systems are highly susceptible to noise, both from movement in the wires and movement between the electrodes and the skin [22]. Pattern recognition systems that perform well in controlled test environments where the user is making isolated movements in a controlled manner often fail to maintain accuracy when adapted to a mobile device that must undergo multiple simultaneous movements. An ideal EMG acquisition system would minimize as much noise as possible in the design. Shortening the wires between the sensors and the signal processing system is preferable. Still, by nature, wearable sensors designed for home use make it difficult to establish good electrode contact with the skin and repeatable positioning [21]. The adoption of pattern recognition-based EMG systems for prosthesis and orthosis control is still a budding field. The current state of the market shows success in using such systems for gross movements (I.E., opening/closing of the hand or a variety of grip positions), but the promise of full robust and naturalistic control has still yet to be realized [17].

1.6 The Orthosis

Compared to a prosthetic, which aims to replace a body part, an orthosis instead supports a body part. In general, an orthosis is an exoskeletal device aimed at structural bracing or aid in movement, commonly used in various biomechanical rehabilitation scenarios [23]. Their rehabilitation potential is often most effective when coupled with physiotherapy techniques. From simple braces to complex research devices with active components, orthoses can vary wildly in design and complexity.

The stroke rehabilitation orthosis in development at CBPR results from several previous theses in this line of development, the most recent of which being Kilborn and Lövgren [3]. It is a left side, upper limb orthosis with one degree of freedom (elbow flexion/extension) actuated by a servo motor, as seen in image 1.2. The end goal of this line of research involves bringing a variety of concepts together into one cohesive device. Myoelectric pattern recognition from BioPatRec is used to decode muscle volition of the elbow joint in flexion or extension using EMG signals, and the orthosis incorporates gravity compensation and assist-as-needed movement into the execution of gamified rehabilitation exercises. The entire system is intended to be a take-home solution for stroke patients with chronic symptoms who no longer receive personalized care from the medical system.

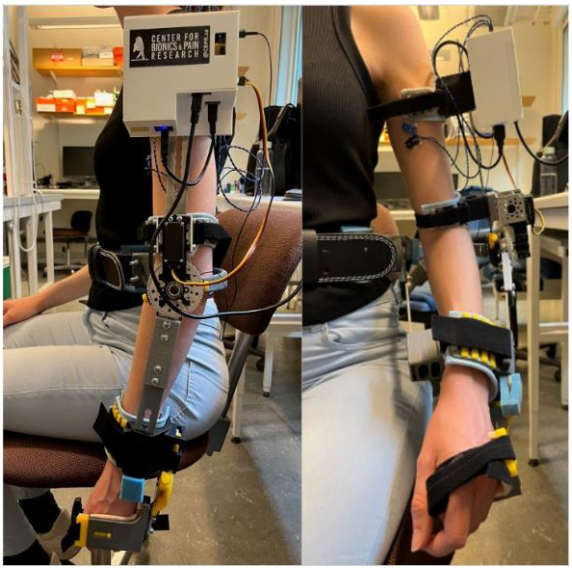

Figure 1.2: The orthosis as it existed at the beginning of this project [3].

By the end of the latest thesis cycle, the design was in a state that showed promise but still had some technical hurdles to overcome before it could be an effective tool. It succeeded as an active orthosis, but could not incorporate gravity compensation or assist-as-needed functionality into the elbow actuation. There were also issues with the training of the EMG classifier not translating well when performing the rehabilitation exercises because the wearer could not wear the orthosis during the

training process. The device was not applicable to patient testing for rehabilitation exercises, and further development was needed.

1.7 Control Theory

In industrial applications, the term "control" refers to methods of regulating the behavior of dynamic systems [24]. This applies to systems where the design desires a stable and responsive behavior of a process variable within the system, such as the temperature of a fluid or the speed of a motor. To achieve this, a controller is implemented into the system that attempts to match the process variable to some reference input.

A common way to achieve stable and responsive behavior of a system is to use a PID controller in a feedback loop. A PID controller incorporates (P)roportional, (I)ntegral, and (D)erivitate terms when calculating the correct system input to match the process variable to the reference. Tuning these three terms allows the system to have desirable response characteristics such as stability, damping, and noise rejection.

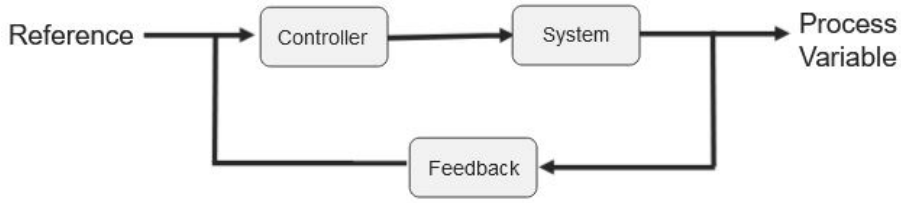

Figure 1.3: An idealized depiction of a feedback loop.

1.8 Gravity Compensation

With EMG signals, it is possible to make a control scheme that, based on the patient's intended action, can assist the patient in moving their arm by compensating for the force of gravity. The goal of gravity compensation techniques is to diminish or remove the need to activate the muscles to counteract gravity, allowing rehabilitation exercises to be performed with the muscle(s) in isolation [9]. Various gravity compensation techniques have been used in upper limb orthoses to reduce the effective weight of the limb and device as experienced by the user. These techniques can be broadly categorized as either active or passive. Active techniques involve using motors or other actuators – usually in conjunction with some position or angle feedback such as an encoder – to apply the necessary torque to the joint to counteract gravity. This has been successfully done using motors with PD feedback control [25], which can be made fast and accurate enough to eliminate the effect of gravity on the limb as it is moved about. Adaptive sliding mode control has also been used to overcome uncertainties in the system parameters [26]. However, purely active systems require high-torque motors that can quickly make the device bulky and heavy.

Passive gravity compensation lacks the fine control and adaptability of a well-tuned feedback control system but can be employed to reduce the torque needed for specific movements, often by counterbalancing the weight of the arm [9]. Constant-force springs can also be used to center the required torque around zero, thereby reducing the maximal torque needed to articulate the joint [27]. This method can work in conjunction with active control by reducing the motors' requirements to actuate the device.

1.9 Assist-As-Needed Control

The last relevant rehabilitation technique to cover is Assist-As-Needed control. This control scheme involves using the minimum robotic intervention necessary to aid the patient in completing the rehabilitation exercise [28]. Many stroke patients struggle to perform the rehabilitation exercises unaided. However, too much aid often results in slacking and a subsequent reduction in the effectiveness of the rehabilitation [29]. A control scheme that exerts just enough aid to the limb to allow the patient to complete the movement is, therefore, optimal for maximizing rehabilitation benefits [28]. This can be accomplished differently between

1.10 The Project

The goal of this project was to take the most recent design of the orthosis and iterate it towards the final vision of an effective stroke rehabilitation device: a solution for stroke patients with chronic symptoms that can go home with the patient and integrate with the BioPatRec platform and the serious gaming system also in development at CBPR. To that end, the main project goals were as follows:

1. Implement gravity compensation and assist-as-needed functionality into the elbow actuation.
2. Implement some means for the device to be worn while training the EMG classifier so that the BioPatRec model translates well to rehabilitation exercises.
3. Improve upon the physical design of the orthosis by reducing play, increasing comfort, and making it easier to don with one hand.
4. Investigate adding a second degree of freedom in wrist flexion and extension.

Implementing these goals involved hands-on prototyping and development of the orthosis. The workflow for this involves various engineering tasks such as CAD work, 3D printing of parts to test, development of a new program for the Arduino microcontroller and MATLAB GUI, and researching and purchasing components as necessary. As individual parts of the orthosis are developed, they were tested for viability. Those results indicated whether the design needs another pass or is ready to be integrated into the larger whole of the orthosis. Overall, the GANTT chart, see appendix A.1, guided the intended workflow and imposed internal deadlines set by the team. Able-bodied participant testing was performed at the end of the project, where the orthosis was evaluated as a cohesive device for its potential as a stroke rehabilitation tool.

2
Methods

This process towards the fulfillment of the project goals will be outlined in this chapter. The project started with a literature review to get an understanding of the field and a variety of subjects relevant to this direction of development. This knowledge shaped further development of the orthosis into the new version, as will be described.

2.1 Literature review

The literature was collected by searching through scientific databases, primarily using google scholar. Selective search terms were employed to find relevant articles. The terms used included but were not limited to 'stroke rehabilitation', 'virtual reality', 'gamification', 'gravity compensation', 'orthosis', 'exoskeleton', 'EMG', 'electromyography', 'electrode placement', 'synergistic movements', and 'slacking'. In addition, normal searches were conducted when more generalized knowledge was needed, such as basic knowledge about strokes or on different types of motors. In the absence of the foundation of trustworthiness established by the scientific process, these sources were chosen with additional care that they were reliable for the scope of their use.

2.2 Requirements

When designing a medical device for home use, it is important to consider the ease of use for the patient, especially for older patients that might not be too versed with technology [30]. Keeping user-centered design in mind is an important approach to making a successful product. Even though the orthosis will eventually be used at home, little to no consideration for ingress protection was made during the prototyping phase. Since the orthosis is still in the early prototype stage, the focus was on making it function better, whereas later improvements to enable at-home usability were not a priority.

The current orthosis is not based on patient feedback, and most mechanical improvements reduce play and make it more structurally sound. Since the active orthosis had not been tested by patients by the start of this project, there was no feedback available other than that provided by healthy participants. Attempts were made to simulate the reduced motor function of a stroke patient while donning and doffing with one arm limp. However, some compensating with the arm was

inevitable due to the nature of the simulation. This does not accurately depict a patient case but gives the group an indication of some shortcomings of the orthosis.

The orthosis is adjustable both based on the length of the patient's arm, as well as the diameter of it. This customization should allow for a good fit for all patients. This is especially important since there needs to be space for electrodes that need a specific connection point on the muscles to read the right EMG signals. These electrodes enable control of the movement via the BioPatRec system developed at CBPR.

2.3 Orthosis Component Manufacturing

Since the design builds on an existing prototype, most of the work was centered on improving the existing components and making the orthosis work with the new parts. Most components are made of 3D-printed Polylactic acid (PLA), resulting in the ability to make quick iterations to ensure the parts function as intended with proper dimensions and tolerances. The parts that are structurally important for the mechanical stability of the orthosis are made of aluminum which has been cut to shape with a Computer Numerical Control (CNC) water jet cutter.

2.4 Torque Requirements

The previous thesis includes a theoretical estimation of the torque needs of the motor, which resulted in an estimated torque of 6.6 Nm [3]. Torque estimations were recalculated in the pursuit of a more robust model and a better understanding of the forces present. Generally, torque is calculated as a rotational implementation of Newton's second law:

$$\tau = I \cdot \alpha \tag{2.1}$$

where τ is the torque, I is the rotational moment of inertia, and α is the rotational acceleration. For the elbow joint, there are two torques to consider: the required torque to counteract gravity and thus achieve gravity compensation and the required torque to execute a rehabilitation movement needed to achieve assist-as-needed control in the case of no user input.

To define an idealized movement upon which to base calculations, the same parameters were used as in the previous thesis - completing a 90°move in one second. Representing the move as a constant acceleration followed by a constant deceleration as shown in Figure 2.1 results in a maximum acceleration of $\pm 2\pi$ rads/s^2.

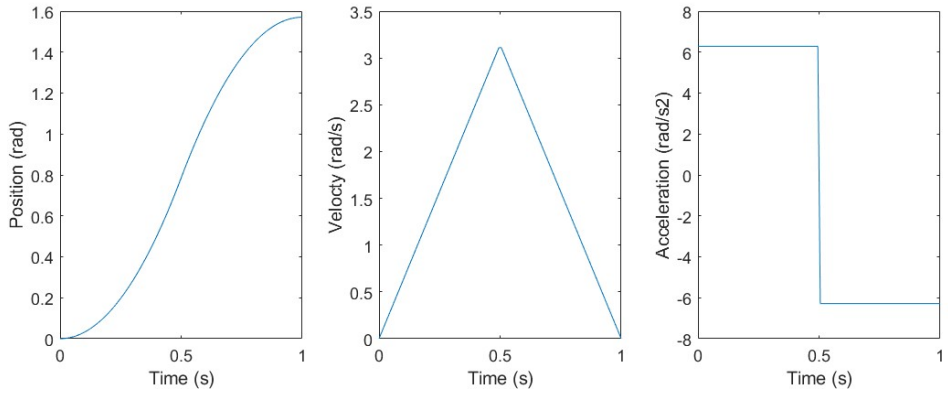

Figure 2.1: Position, velocity, and acceleration profiles for an idealized movement of the elbow joint during assist-as-needed functionality.

For calculation purposes, the lower part of the orthosis is modeled as an evenly distributed weight of $m = 0.52$ kg with a length of $l = 0.40$ m [3]. This gives a rotational inertia of:

$$\begin{aligned} I_{orthosis} &= \frac{1}{3}ml^2 \\ &= \frac{1}{3}(0.52)(0.40)^2 \\ &= 0.0277 \text{ kgm}^2 \end{aligned} \tag{2.2}$$

The rotational inertia of the forearm and hand around the elbow are 0.027 kgm^2 and 0.067 kgm^2 respectively [31], for a total of 0.0943 kgm^2. Thus the torque requirement to perform the idealized movement is:

$$\begin{aligned} \tau &= (I_{arm} + I_{orthosis}) \cdot \alpha \\ &= (0.0943 + 0.0277) \cdot (6.28) \\ &= 0.764\text{kgm}^2 \end{aligned} \tag{2.3}$$

The torque requirements to perform gravity compensation are modeled as the torque necessary to achieve zero acceleration. In theory, this is the moment exerted on the joint by the arm's weight and orthosis. The lower part of the orthosis weighs $m_{orthosis} = 0.52$ kg with a center of mass $r_{orthosis} = 0.15$ m from the joint. Likewise, $m_{forearm} = 1.62$ kg, $r_{forearm} = 0.138$ m, $m_{hand} = 0.61$ kg, and $r_{hand} = 0.40$ m. Therefore the maximum torque requirement to accomplish gravity compensation is:

$$\begin{aligned} \tau &= \sum Grm \\ &= G \cdot (r_{forearm} \cdot m_{forearm} + r_{hand} \cdot m_{hand} + r_{orthosis} \cdot m_{orthosis}) \\ &= 9.81 \cdot (0.138 \cdot 1.62 + 0.40 \cdot 0.61 + 0.15 \cdot 0.52) \\ &= 5.35\text{Nm} \end{aligned} \tag{2.4}$$

Adding these values together gives the maximum torque the orthosis might need to exert during normal operations:

$$\begin{aligned} \tau_{max} &= \tau_{assist} + \tau_{grav} \\ &= 0.76 + 5.35 \\ &= 6.11\text{Nm} \end{aligned} \tag{2.5}$$

Notably, this is close to the theoretical estimation in the previous thesis (6.6 Nm [3]). This number relates to the scenario of hypothetical maximum torque – when the forearm is horizontal and moving upwards, and assist-as-needed functionality is supplying 100% aid. The gravity compensation component of torque varies as a function of the angle between the orthosis and the ground, and the assist-as-needed component varies between the acceleration and deceleration parts of the movement.

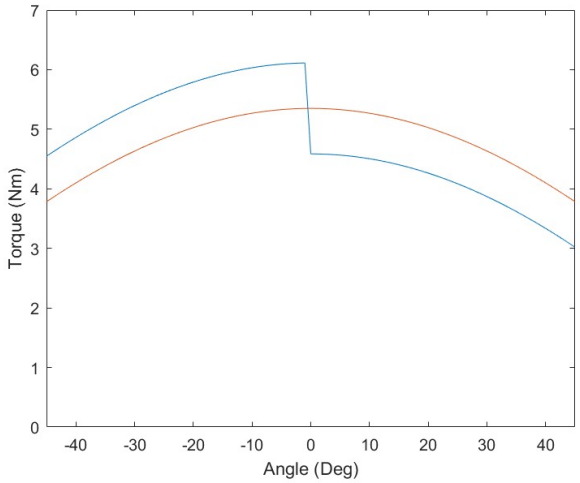

Figure 2.2: Elbow joint torque for an idealized movement from 45°below the horizontal to 45°above. Shown for gravity compensation (red) or for gravity compensation with assist-as-needed (blue).

How the torque requirement changes across the execution of a move can be seen in Figure 2.2. While torques up to an estimated 6.11 Nm are possible, the majority of the rehabilitation runtime does not require maximum torque. Likewise, there is a theoretical use-case where the torque requirement is negative: when the forearm points straight down and the user is attempting to accelerate in the negative direction. In expected use, it is unlikely for these two situations to coincide, yet it is prudent to design around torque requirements that may extend to the negative maximum assist-as-needed torque, -0.76 Nm.

This theoretical model has limited application to practice, as there are significant other forces that are difficult to model. Any actuation system brings its own rotational inertia as well as static and kinetic friction, none of which are generally available information for commercially available actuator systems within the budget of this project. There is also a force on the joint applied by the arm due to the misalignment of the rotational axis with the user's elbow. Ultimately, these calculations suffice for a rough estimate for sourcing parts but have limited

application to the actual kinematics of the system.

2.4.1 Wrist Joint Torque Requirements

Regarding the wrist joint, the equations are largely the same as for the elbow, with different parameters. The difference is that the wrist does not need to compensate for gravity since it moves horizontally. The inertia of a hand, through some simplifications, is estimated to be 0.0006 kg m^2 [32]. When estimating the inertia for the hand assembly of the orthosis (seen later in figure 2.16), the easiest approach is to take the same inertia of the human hand and copy that number. This should be an overestimation of the inertia since the weight of the hand-supporting subassembly of the orthosis is roughly 0.2 kg compared to the 0.6 kg of a human hand. The weight distribution is assumed to be fairly similar as a simplification of the calculations. The angular acceleration that the orthosis will be moving at is $2 \cdot \pi$ rad/s^2, this leads to the following equation for torque:

$$\begin{aligned} \tau &= (I_{xort} + I_{xhand}) \cdot \alpha \\ \tau &= 2 \cdot I_{xhand} \cdot \alpha \\ \Rightarrow [kgm^2/s^2] &= [kgm^2] \cdot [rad/s^2] \end{aligned} \tag{2.6}$$

When inserting values:

$$\tau = (2 \cdot 0.0006) \cdot 6.14 = 0.0074[Nm] \tag{2.7}$$

The wrist joint torque is negligible compared to the elbow torque due to the smaller weight and lack of a gravity compensation component. This also results in a general use case that varies evenly between +0.0074 and -0.0074, unlike the elbow joint, which necessitates actuation that can apply force in both directions reliably.

2.5 Actuation

The preexisting device uses a servo motor to control the elbow joint [3]. Servo motors, such as the one used, are DC motors packaged as a unit with a feedback controller, giving the user precise control over the position of the motor [33]. Generally, the servo receives a pulse width modulated (PWM) signal where the pulse width corresponds to a position along the servo's range, and the internal circuitry relegates the correct current to the motor to send it to that position. This is accomplished via feedback control that is usually not accessible to the user without tampering with the module, as such, the servo will output up to the maximum torque available to achieve the target position. The motor used in the orthosis is a central decision upon which the entire control strategy and capabilities depend. With this in mind, a table containing some of the orthoses proposed by previous research is presented below to compare motor type with controllability.

Table 2.1: Different orthoses created, showing joints moved, type of actuator used and control type.

Citation:	Joint:	Actuator:	Control:
[19]	Elbow	Brushed motor	Position control
[20]	Knee	Brushed motor	Position control
[25]	Shoulder, elbow	Brushless motor	Gravity compensation
[27]	Upper limb	Servo motor	Gravity compensation
[34]	Elbow	Linear motor	Gravity compensation
[35]	Shoulder, elbow, wrist	Stepper motor	Gravity compensation
[36]	Elbow, wrist, fingers	Servo motor	Position control

The current servo motor in the orthosis is used for position control [3]. With some reconfiguration and the addition of springs, servo motors have succeeded in accomplishing gravity compensation [27]. However, this limits the application from being used as 'assist as needed'. As seen in table 2.1, there are several ways to achieve gravity compensation, meaning there is no limitation to what type of motor must be used. Brushed [20] and brushless [25] motors can use in tandem with control systems to achieve gravity compensation or position control. Brushless motors generally offer better performance, less noise, and longer operation life compared to brushed motors [37]. However, most commercially available driver boards come prepackaged with sophisticated control to achieve position- or speed-based output, which either needs to be worked around or deconstructed to produce torque-based output. Brushed DC motors, on the other hand, only require an H-Bridge and transistor/MOSFET to control and have a linear relationship between the input voltage and output power.

To implement a control strategy that can achieve aim (1), the actuation of the orthosis elbow joint must be torque-controlled instead of the previous position control. The previous servo motor could potentially be repurposed to tighten/loosen a spring as necessary to put torque on the joint. This design comes with a few disadvantages:

- The motor would only be able to apply force in one direction, which, while sufficient for gravity compensation, would not cover all cases of the assist-as-needed functionality.
- There would still need to be a way to mechanically disengage the motor during the calibration process.
- The main advantage of this method, reusing the existing motor, does not scale if copies of this prototype are eventually built.

There are other alternatives to motors that could be explored, such as pneumatic or hydraulic actuators [38]. However, these have not seen as much successful implementation in orthoses, while electrical motors are the most common. Both pneumatic and hydraulic systems suffer from similar drawbacks. Namely that they are generally not very compact, largely inefficient, and would only be suitable for applications that require low to no portability. The pneumatic and hydraulic cylinders themselves are not the biggest issue, but rather their reliance on pressure supplies to work.

The decision was made to use brushed DC motors for both the elbow and wrist due to the expected ease of implementation, along with being easily reversed or passively driven. The MOT-I-81573-30-27 from ISL[39] was chosen for the elbow based on the rated torque, speed, and power. The wrist torque requirement is sufficiently small that motor strength is not a limiting factor - since there are simplifications taken during the calculations, it was decided to opt for a drive train with more torque than the calculated 0.0074 Nm, while not having too high torque since that would reduce the resolution of the control scheme. The 238-9715 from RS Pro [40] was chosen due to its low weight, size, and price. This motor has 0.0058 Nm, but will be geared with a 4:1 ratio, effectively allowing it to output 0.023 Nm, which is sufficient for the cause.

2.6 Motor Control

Replacing the previous servo motor with a brushed DC motor allows for more direct motor control. The motor has a linear relationship between input voltage and output power which allows it to be embedded in a control loop. With a microcontroller controlling the motor input signal and reading the output speed with an encoder, a digitally implemented PID controller offers greater flexibility of control than the previous servo motor. This allows the motor to operate in position-based feedback control, such as the servo, but also switch to speed-based feedback control or even feed-forward control as the situation necessitates.

To accomplish gravity compensation, a calibration sequence was developed that calculates the required motor input to achieve equilibrium as a function of elbow joint position. This is done by instructing the user to relax their arm while the orthosis sweeps between the endpoints at a controlled speed and records the torque needed to maintain the speed at various points. Different methods for data collection and model fitting were explored to find a calibration process that results in a functional gravity compensation model.

Assist-as-needed functionality was done by interfacing with the BioPatRec protocol and parsing serial communications for commanded moves, then progressively adding torque to the motor until the move was accomplished. That was done with speed-based feedback control. However, the control algorithm was critical to creating the requisite response. Unlike the majority of control applications, the goal with the assist-as-needed functionality is not to match the motor speed to the reference speed as quickly as is stable but to slowly ramp up the assistance so that the user has a moment – roughly half a second – to attempt the move with minimal aid from the orthosis. Different PID tunings and delays/-pauses of the PID controller were explored to create suitable assist-as-needed action.

The MatLab GUI was overhauled to provide the user with an interface for calibration and setup of the orthosis. The GUI also provides manual control, a variety of settings that can be changed, and functions as a troubleshooting tool. Actual rehabilitation

exercise is performed through the BioPatRec GUI. However, the orthosis' custom GUI is still necessary to coordinate calibrating the gravity compensation model and set-up for the rehabilitation exercise session.

2.7 Reducing Backlash

Backlash or play is a common issue in mechanical systems that manifests whenever the transmission link has a gap [41]. This is something that would negatively affect the control scheme of the motor since it is fairly prevalent when changing motor direction. It would also lead to wear and tear since the components would grind against each other, which could have major complications in the long run. This caused some issues with the orthosis while tuning the controller, which led to the need to replace the gears since they got worn out from the tuning. This issue should not be as prevalent during actual use since the forces exerted should be lower and less spastic compared to the tuning.

In extreme cases, backlash can also introduce an unwanted delay, as parts with a gap would take time to engage with each other. It is, thereby, important to design the components with minimal tolerance to ensure a good fit and increased accuracy of the orthosis as a whole. A considerable amount of effort went into making prototypes to test the tolerance needed for the final component before printing it. Since the orthosis is still in a prototype stage most parts are made of 3D printed PLA which can be easily changed and printed new if found to be not perfectly suitable.

2.7.1 Reducing Backlash in Sliders

One major reason for backlash in the orthosis was the fact that it was difficult to tighten the old upper shoulder strap with just one hand. Since the orthosis is intended to eventually be used at home, it is important to think about the end user being able to don it without any help, if possible. Instead of using Velcro straps, the new prototype features a ratcheting mechanism which makes tightening a lot easier, ensuring less play in the system as a whole. This led to redesigning the sliders to accommodate the attachment of the ratcheting device, see figure 2.3 for the attached ratcheting mechanism. This attachment process was a bit of a back-and-forth with several prototyping stages before a snug fit was achieved. Furthermore, it supports comfortable padding to reduce pinching risk, and increase comfort. The new sliders provide a tighter fit and still allow for access to place electrodes on the biceps- and triceps brachii as well as the forearm.

One downside with the sliders is that they are longer, which makes the arm of the participants no longer centered. This issue looked different for different participants, where some were pushed more outwards while others were pushed more inwards. The reason behind the sliders needing to be longer is to fit the ratcheting device. An easy solution to this would be to extend the sliders on the opposite side of the attachment point for the strut, thus not altering the arm alignment.

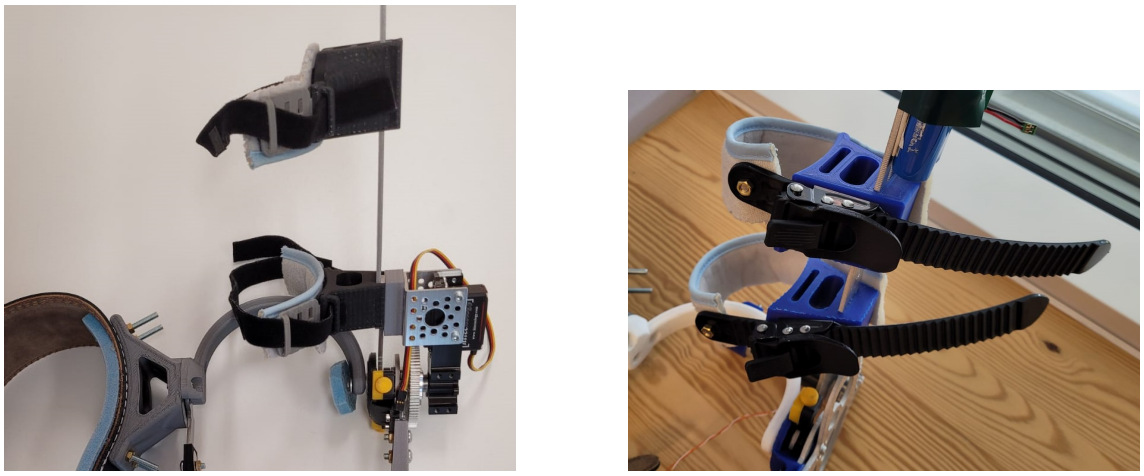

Figure 2.3: Comparison of the old and new upper arm attachment. On the left: Picture of the old attachment style where velcro straps were used on the upper arm On the right: Picture of the ratcheting devices connected on the orthosis

The lower slider of the upper arm is now angled to better allow electrode placements on the bicep brachii of the patient. This change was made due to the fact that the gear sticks out more than previously due to the new gear ratio, leading to the need to move the slider away from the gear while still providing a snug fit for the patient. See figure 2.4 for how the new slider looks.

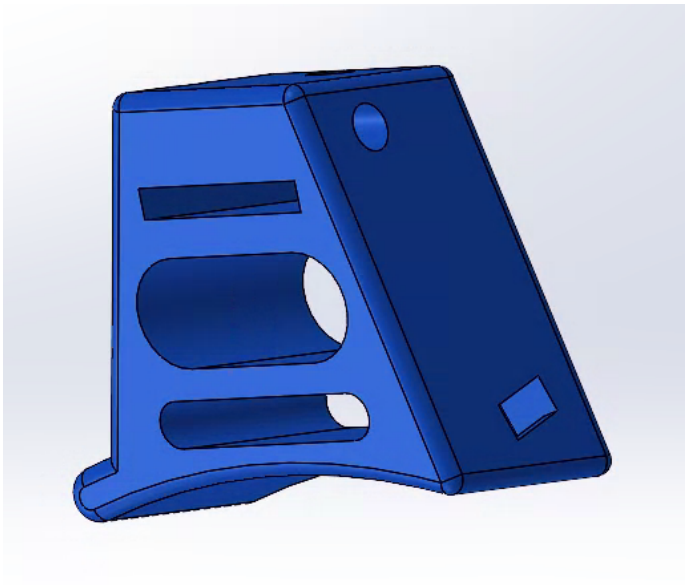

Figure 2.4: Lower slider for bicep, where both the ratcheting device attachment and the angle of the slider can be seen

The new sliders are also made to work with a different type of strut, and will not feature the old design of a compliant mechanism that the user could press down to change the attachment point for the orthosis to the patient, see figure 2.5 for a comparison with the old and new slider design. This old design featured a lot of

play to it and was thereby reworked. The new design is fastened with a nut and bolt, making it possible to adjust to any part along the groove of the strut. These new sliders also include the attachment for the ratcheting device. With this, a new strut design was made, which will be discussed in chapter 2.7.2.

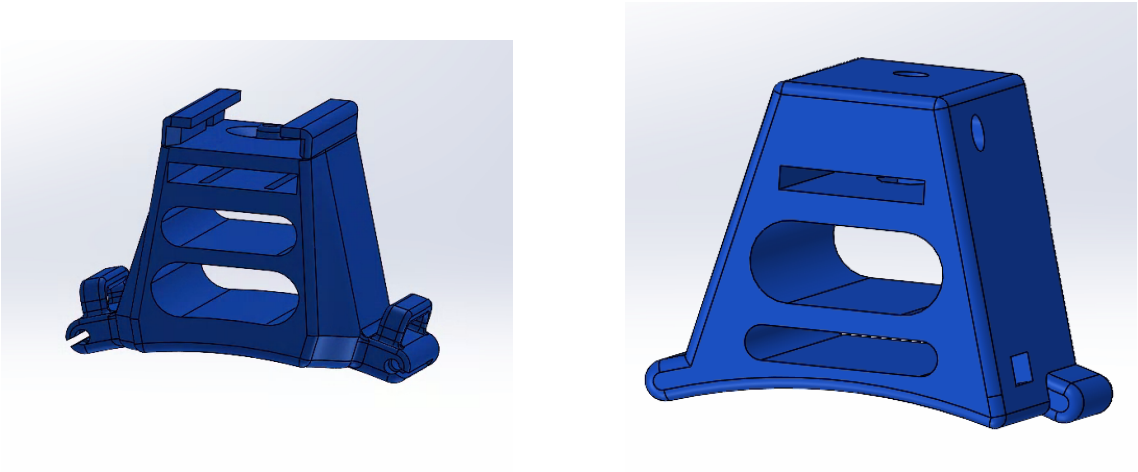

Figure 2.5: Comparison of the old and new upper bicep slider. On the left: Old design, where the compliant mechanism can see at the top of the slider, as well as hoops for the old velcro straps can be seen on the sides. On the right: New design, where the bolt hole is visible on top, as well as the attachment for the ratcheting device on the right side.

2.7.2 New Struts to Reduce Backlash

The new struts are made of one solid piece of aluminum, compared to previously where two pieces were linked together with a 3D-printed linkage. While the old solution of attaching two metal struts did not include much play, the decision to make the struts into one part was made. This was justified based on the fact that the new sliding mechanism that was decided on needed a different type of groove in the strut. The new sliders will be fastened along the strut with a nut and bolt, which limits the amount of play in the system compared to the old solution. See figure 2.6, for the differences between the new and old wrist strut designs.

Figure 2.6: Comparison of the old and the new wrist struts. On the left: Old design, where it was made of three parts and the old groove with incuts. On the right: New design, where it is just one piece, and the groove is straight, also added bolt holes for better attachment with the gear can be seen to the right in the figure.

Other struts also got reworked, such as the upper arm strut, which now features a mounting place for the motor, and can be seen in figure 2.7 compared to the old

strut design. While the new design is largely the same, another key difference can be seen, namely that it is just one part, as compared to three with the old design.

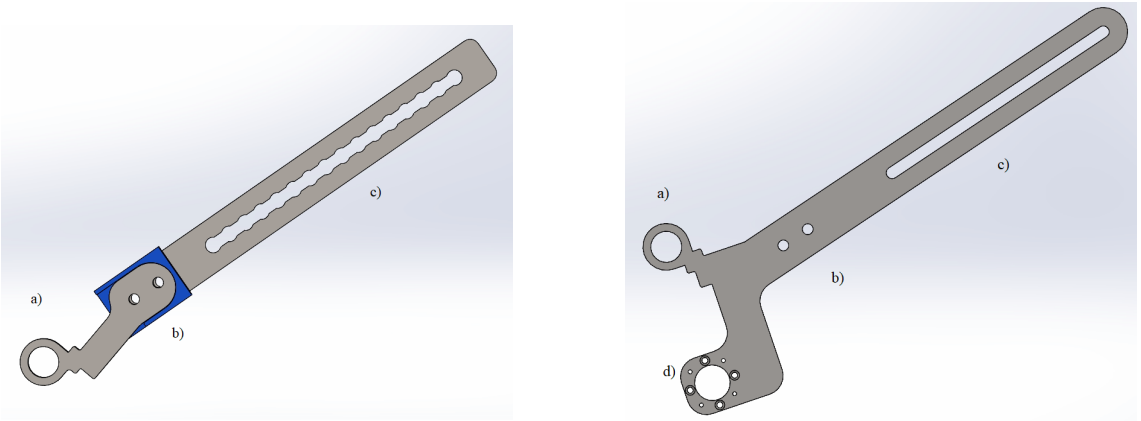

Figure 2.7: Comparison of the old and the new upper arm struts. On the left: Old design, a) is the attachment for the roll-bearing that allows rotation in the elbow joint. b) an attachment point for the two different metal parts, seen in blue. Also where the lower bicep slider is attached c) shows the groove where the upper arm slider attaches. On the left: New design, a) is the attachment for the roll-bearing that allows rotation in the elbow joint. b) is now just for attaching the lower bicep slider. c) a new groove that allows the upper arm sliders to be attached at any point along the groove. d) added motor mount.

2.8 Elbow Drive-Train Improvements

The different components of the elbow drive-train that were changed due to various changes in the structure of the orthosis will be presented here.

2.8.1 Elbow Motor Mount

There are some drawbacks besides the backlash in the previous iteration, such as the motor not being back-drivable or able to do torque control. This led to a new motor being decided on. The decision to use another motor led to redesigning the mounting of said motor, as well as the gearing needed. Due to the bigger size of the motor, it was decided to mount it underneath the orthosis at the U-shaped support instead of sticking out as with the previous design. See figure 2.8 for a picture comparing the old and the new system. This also meant some slight changes if the metal struts needed to be done to enable the attachment of the new motor, which was discussed in chapter 2.7.2.

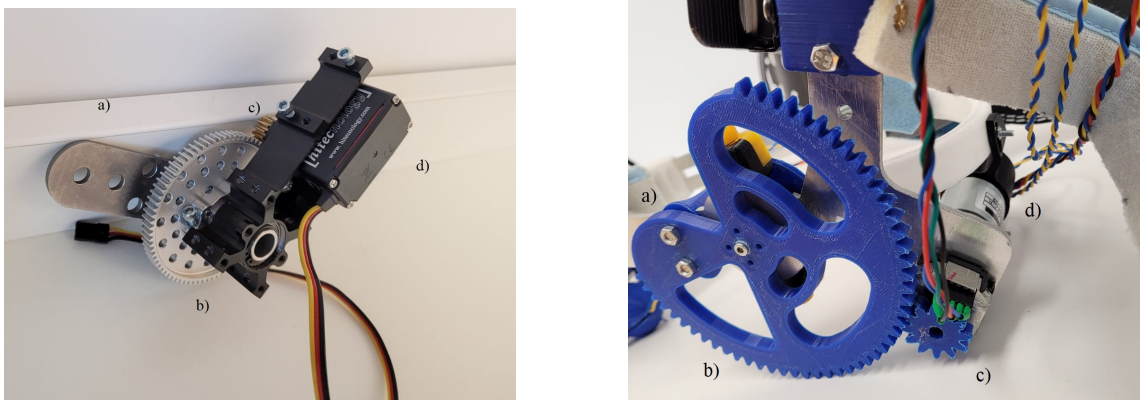

Figure 2.8: Comparison of the old and the new motor attachment. For both pictures: a) facing towards the wrist, b) big gear, c) small pinion gear, d) motor.

2.8.2 U-Shaped Elbow Support

The U-shaped support, among other things, helps the patient to keep their arm away from their body. It also works as the pivoting point for the elbow motor, allowing flexion and extension of the elbow. This new attachment also allows the creation of a connection between the U-shaped support and the motor, as well as protecting the wires that attach to the back of the motor. This would also stabilize the motor and prevent it from unintentional movement. The motor is mounted far enough away from the U-shaped support so as to not interfere with the patient, see figure 2.9. This attachment put pressure on the motor forcing it out of alignment, subsequently making the gears misaligned. This caused some friction when the teeth of the gears were grinding against each other at an unintended angle. After numerous iterations to create this support without interrupting the alignment, it was still not perfect, but it was deemed good enough not to iterate further on, see figure 2.9b for a look at the final iteration of the motor wire cap.

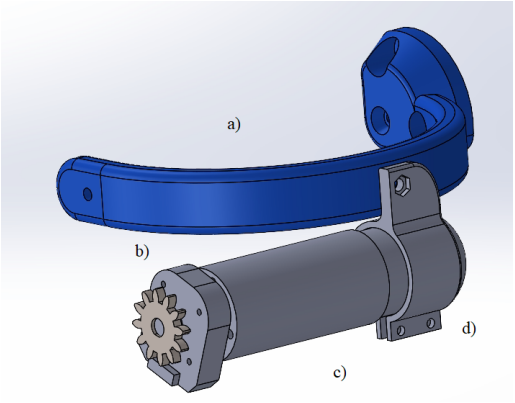

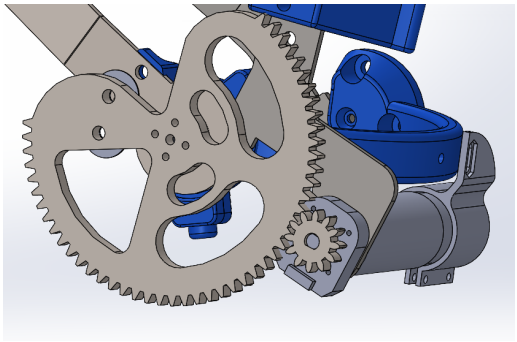

Figure 2.9: Comparing the iterative process of designing the motor cap attachment. On the left: Here the U-shape assembly can be seen. a) is the U-shape support, b) is the encoder with the driving gear connected, c) is the motor, d) is the early design, motor wire cap connecting to the U-shaped support and protecting the wiring. On the right: Motor wire cap iteration, now seen together with the rest of the components, note that the smaller gear should be rotated downwards in relation to the big gear, as to better align the wire cap with the screw hole in the U-shape support

2.8.3 Elbow Gears

The gears are custom-made with a 6:1 ratio, which was necessary to achieve the desired torque from the motor. The gears were also designed to be big enough to move the motor away from the patient to mitigate risks. The choice of 3 mm thick aluminum was made initially based on what material was available at the time, though a thicker gear would be preferred. The thinner gears led to slipping and misalignment due to the gear tooth face width, but it was a limitation due to the material available and the shaft length of the motor. The bigger gear is also manufactured with a few teeth removed to avoid potential pinch points, and since the range of motion corresponds to 150°, it will not affect the orthosis function, see figure 2.10.

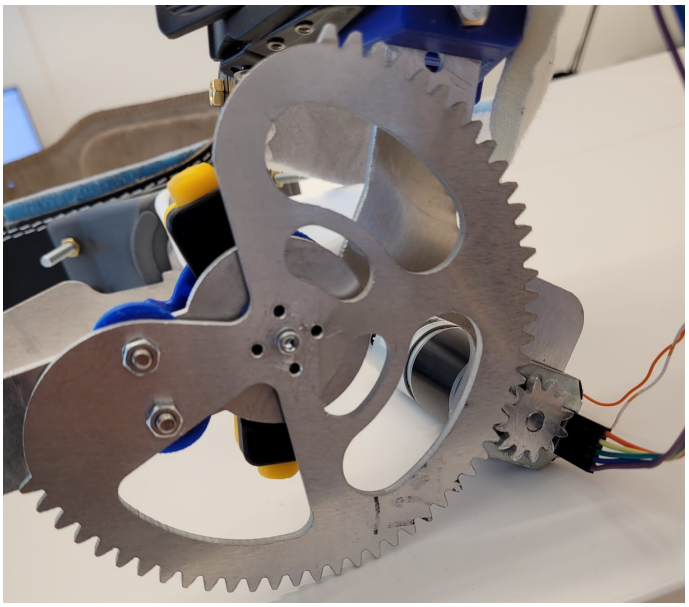

Figure 2.10: The custom-made gears with the intended gear ratio and size, seen attached to the orthosis, early iteration using aluminum

The aluminum used was also rather malleable and became worn quickly, resulting in the D-key on the pinion gear getting worn out over time and causing play while switching the direction of rotation. After experimenting with these aluminum gears, the slipping and misalignment rendered the orthosis unreliable, and the decision to move over to 3D-printed gears with a 6 mm thickness instead was made. This had its own drawbacks since PLA is weaker than aluminum, the D-key of the pinion gear still wore out rather quickly. An idea about having a hub on the pinion was tested. This would spread the force over a bigger area, reducing the pressure, and minimizing the wear, see figure 2.11 for the pinion gear with a hub.

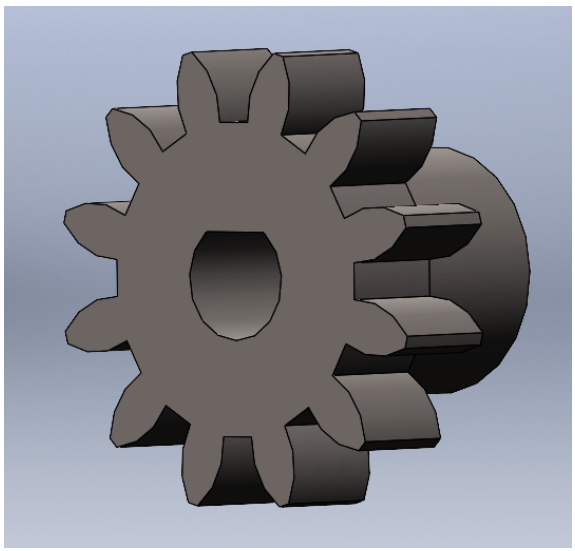

Figure 2.11: Pinion gear with extended hub and D-key profile

2.9 Adding an Active wrist

To be able to rehabilitate the wrist of the patient as well as the upper arm, an active wrist function was added. Similarly to how the elbow joint can be moved, the new wrist joint also moves in flexion and extension. For this, the motor was attached to the adjustable wrist support, see figure 2.12. This assembly comprises four subassemblies, see figure 2.12 on the right for an overview of the parts separately. These subassemblies will be broken down and explained in further detail later in the chapter.

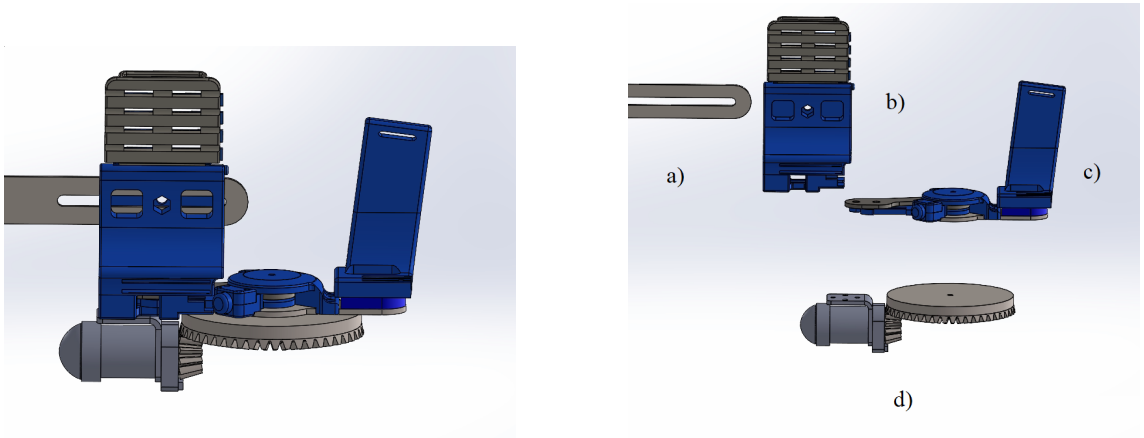

Figure 2.12: Active wrist assembly, both connected on the left, and exploded view on the right. Active wrist assembly, exploded view: a) forearm strut, b) adjustable wrist support, which doubles as a connection point for both the hand assembly and motor assembly. c) hand assembly, d) motor assembly

The beveled gears are visible in figure 2.13, translating the rotation 90°. The decision to use beveled gear was made to make the motor stick out less underneath the orthosis but also at a safe distance from the user. Due to the low torque needed from the motor, the gears are made of 3D-printed PLA and have not experienced any wear. The gear ratio is 4:1, giving the orthosis more torque, both to allow rehabilitation and to resist involuntary spastic movements.

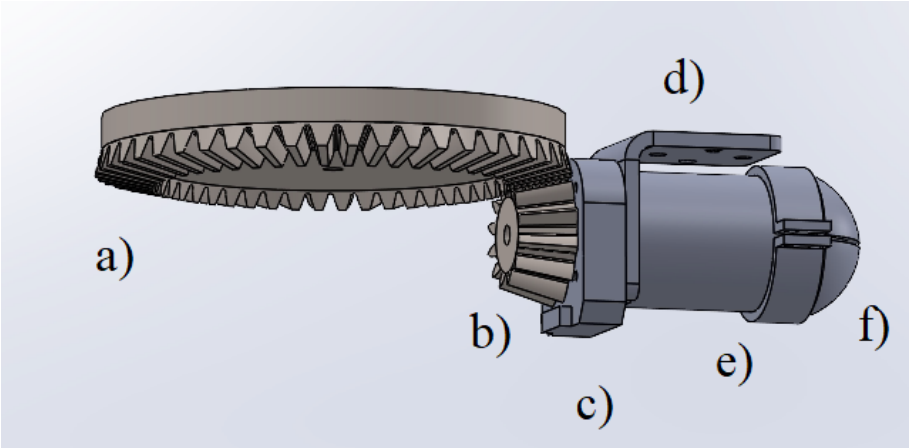

Figure 2.13: Assembly of the active wrist, a) is the big gear connected to the rest of the orthosis. b) is the small gear that drives the big gear. c) is the encoder, d) is the L-bracket that mounts the motor to the adjustable wrist support, e) is the motor, f) is a motor wire cap.

Due to limitations in motor shaft length, it was necessary to use a hub on the gear for it to get connected. Without this, the encoder and gear would not fit along the shaft, and the encoder would not be able to be engaged since the motor shaft and encoder opening were different sized and no encoder collar would work. This led to the decision to make the outer diameter of the hub 6mm to fit with the diameter of the encoder and the inner diameter 2.31mm to fit with the shaft diameter of the motor. However, when 3D-printing parts, it is never that simple since the extrusion of material will spread out a bit, and a very fine precision is hard to achieve. After a few iterations, a snug fit was accomplished, and the assembly was done. See figure 2.14 for an exploded view of the active wrist.

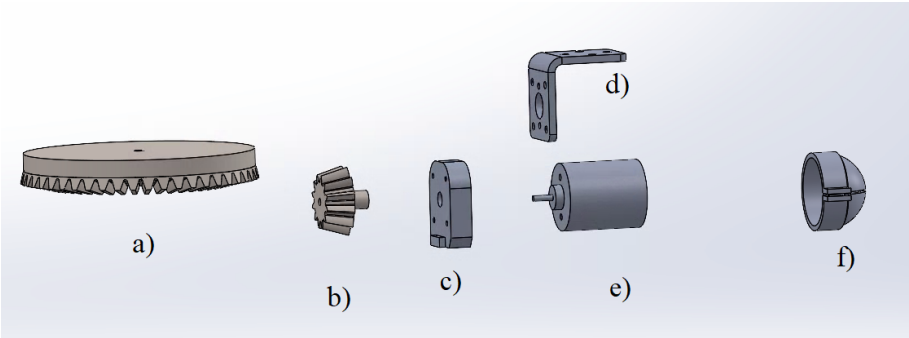

Figure 2.14: Exploded view of the active wrist assembly, a) is the big gear rotating the wrist joint. b) is the small gear that drives the big gear. c) is the encoder, d) is the L-bracket that mounts the motor to the adjustable wrist support, e) is the motor, f) is a motor wire cap.

Furthermore, the L-bracket that is marked as *d)* and can be seen in figure 2.13 and 2.14 is custom-made. Due to high tolerance requirements but low precision manufacturing, the whole assembly had to be adjustable to accommodate the dimensions of this bracket since it would differ from the proposed dimensions. Some steps that

were taken to avoid any issues were to add spacers above the big gear seen as *a)* in the aforementioned figures. This would compensate for the change in the y-axis of the L-bracket. The wrist support also needed to be changed slightly, partly due to the gear taking up some of the shared space and partly to make the attachment of the L-bracket adjustable. To make it adjustable, a groove was added so that the bolts could connect along it, and another groove was added to have a countersunk nut in the wrist support, see figure 2.15.

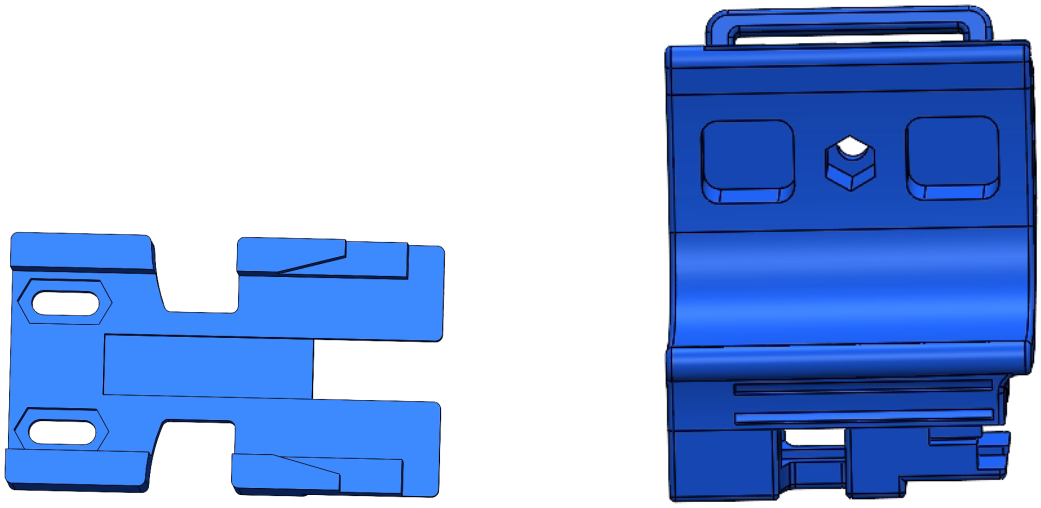

Figure 2.15: Wrist support, both as a whole and section view, seen with hand facing the right of the picture. On the left: Section view of the wrist support, where the countersunk grooves are visible on the left side of the piece. On the right: Wrist support, seen from the side, including where some material was removed to accommodate the bigger gear, seen in the bottom left of the figure.

To accommodate the active wrist, the hand assembly also had to be changed slightly, namely flipping the mechanically adjustable stopper to the top of the point of rotation, see figure 2.16 for a comparison of the old and new assembly. Some more hand support changes were needed to accommodate the switch since the old support would overlap with the locking mechanism. This new hand support design has a shorter base and is no longer adjustable in terms of height. This was scrapped due to being deemed unnecessary since the Velcro strap holding the hand in place is adjustable and would already accommodate a larger hand.

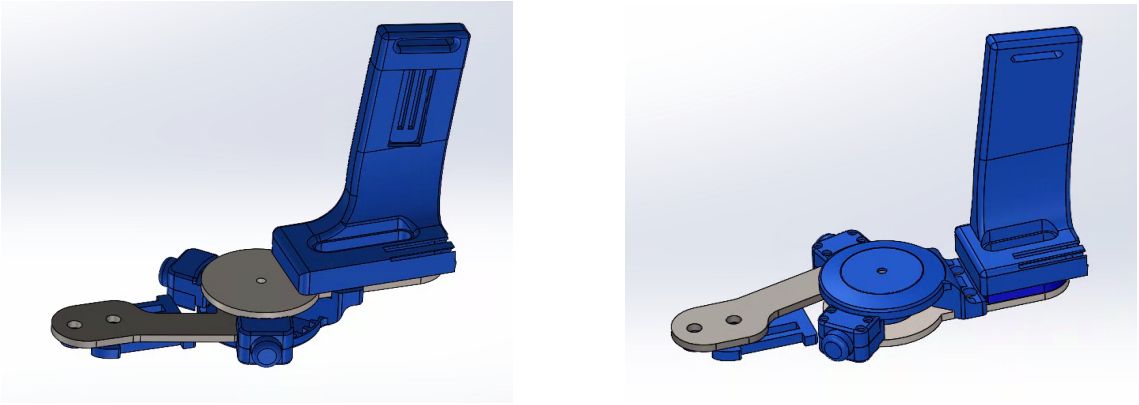

Figure 2.16: Comparison of the old and new hand support assembly. on the left: Old hand assembly, featured adjustable height, based on user hand width. On the right: New hand assembly, notice the spacer and shorter hand support base to not interfere with the locking mechanism.

2.10 Safety Measures

Some safety measures have been considered to reduce risks during the use of this device. For example, a patient with really long hair could get their hair entangled in the motor or gearing. The chance of this can be mitigated by using a hair tie. Still, consideration has been made to minimize pinch points in the design, such as redesigning the driven elbow gear to remove the teeth along the unnecessary portion of the circumference. Wiring between the motor, encoder, and electrical enclosure is also susceptible to pinch points and has thus been made with limited extra length and restrained away from the drive train.

A significant risk is the orthosis pushing the user's limb into a painful position, such as overextending the elbow. There are adjustable mechanical stops at each joint that can be set to the patient's specific range of motion and limit joint movement in both directions, see Figure 2.17. These stopping mechanisms work by pressing the mechanical button of the two adjustable stops so they can be moved between different grooves in the cover. These groves were enforced to improve the lifespan of the mechanism as a whole. The calibration sequence also finds these hardstops and incorporates them as the endpoints of calibration into the control algorithm. The overall power of the motor is also limited not to exceed the necessary torque required for the motion and to minimize discomfort or pain to the user.

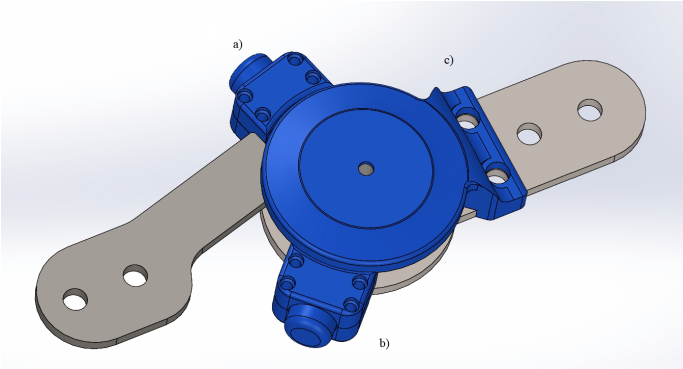

Figure 2.17: Mechanical stop that is adjustable to allow a certain degree of rotation. a) and b) are the two adjustable stops, while c) is the cover that has grooves for the stops to fit into.

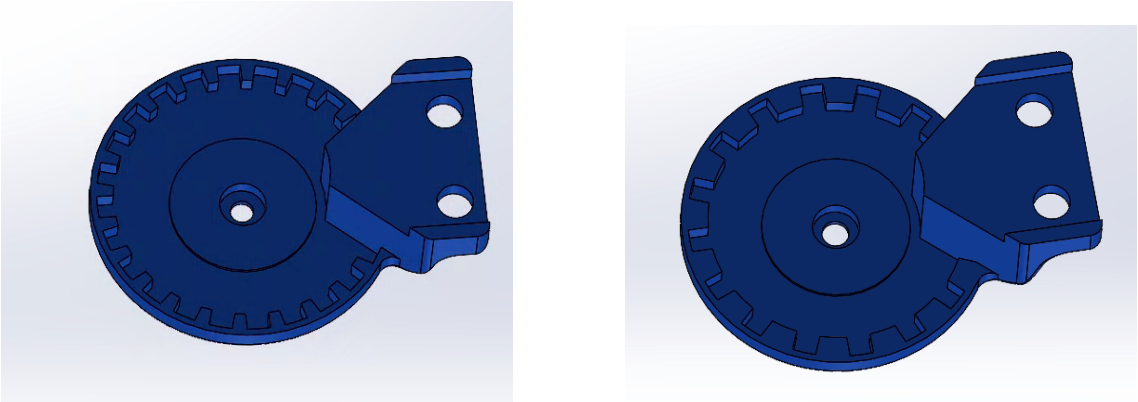

Figure 2.18: Comparison of the old and new hinge covers. On the left: Old cover with smaller but more teeth. On the right: New cover with bigger but fewer teeth, otherwise same dimensions, despite looking smaller in the photo

2.11 Electric

The circuitry to run the motor was overhauled due to the change of motor. The new motor is rated at the same voltage and similar power draw as the servo motor used by the previous orthosis, so the battery did not need to change. However, the switch to a brushed DC motor necessitated additional circuitry to control the motor, and a motor driver board was incorporated into the design. Originally the driver board used was the MAKER MDD3A from Seeed Technolody. This board did not come with overcurrent or undervoltage protection, and several driver boards were damaged in the process of discovering that other components' specifications were misinterpreted or incorrect. Eventually, that model of driver board was replaced with one of higher performance, and the DFR0601 from DFRobot was chosen due to its better ratings and overcurrent and undervoltage protection [42]. Finally, AMT103 encoders from CUI were added to the output shaft of the motors to provide position/speed feedback to the microcontroller [43]. To incorporate these new

elements, changes were made to the circuit design, as shown in figure 2.19. This also required the circuitry to be rebuilt on a new perfboard and the electrical enclosure to be redesigned to accommodate its slightly larger size.

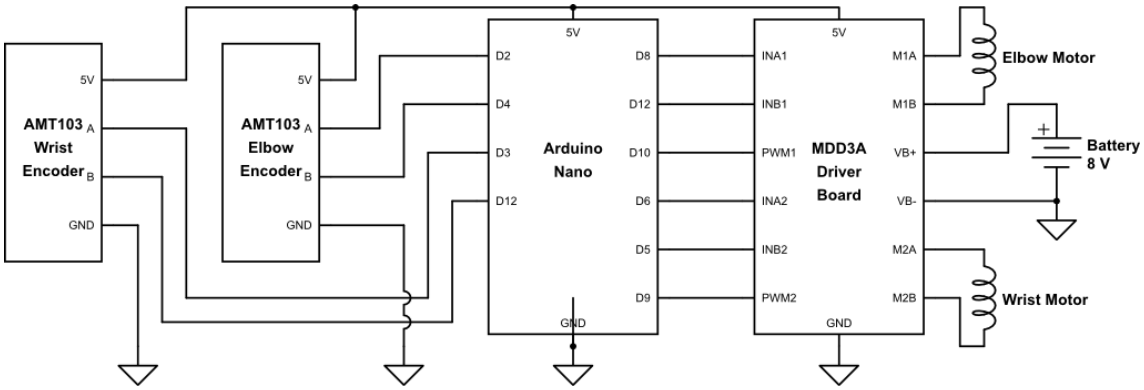

Figure 2.19: Circuit diagram of the system. Covering everything from encoders, motors, battery, driver board, and Arduino. Encoder A and B are the digital feedback of the encoder quadrature signal, from which relative position is calculated. For each motor, the driver board takes two digital signals (INAX and INBX) to determine direction and one PWM signal to determine output current.

Actuating the motors creates an audible whine at the frequency of the PWM signal. While this whine does not affect performance, it is sufficiently loud to cause discomfort to the user and negatively impact perception of the orthosis. The Arduino Nano has six pins capable of producing a PWM output signal, however they do not all share the same base frequency and are tied to different clocks within the registers [44]. Pins 9 and 10 were ideal, as the clock registers could be altered to increase the PWM beyond the human audible range without compromising the timing logic and, thus, serial communications. With the change to the DFR0601 driver board, each motor needs a single PWM signal for the speed and two digital signals to control direction, both wrist and elbow motors could be driven using PWM pins 9 resp. 10.

The encoders require two digital pins each and achieve higher performance when using interrupt pins, but the Arduino Nano has only two interrupt pins (pins 2 and 3). Due to this limitation, one interrupt pin and one digital pin were used for each encoder, which was found to achieve sufficient accuracy of position feedback for this application.

2.12 Programming

A robust and reliable controller was needed for actuating the motor during the calibration sequence to generate the gravity compensation model, as well as for

the Assist-As-Needed functionality. It was initially done using a library called PID.h in the Arduino software. The library creates a PID controller that matches an output to the user-defined reference by using the configurable Kp, Ki, and Kd tuning parameters. Motor functionality was separated into two modes: position and speed. In position mode, the PID takes the encoder position as the process variable and attempts to match it to the input reference. In speed mode, the process variable is instead the angular velocity of the elbow as estimated from the encoder's position feedback. To obtain an accurate and responsive speed estimation, several different estimation methods were tested to find an ideal balance between responsiveness and accuracy. A discrete filter was developed as shown in Figure 2.20.

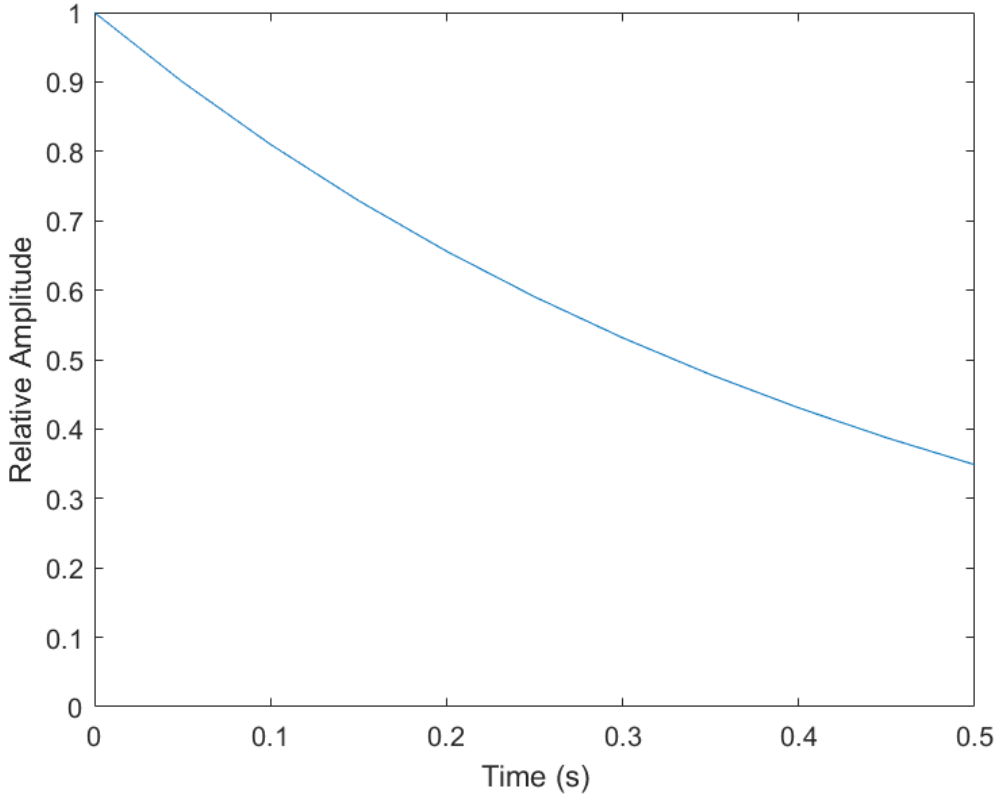

Figure 2.20: The impulse response $h(t) = 0.9^{t/0.2}$ of the discrete low-pass filter used to smooth out the encoder speed estimation. Sampled with a time step of 50 ms.

In practice, integrator windup was found to be a significant issue with the imported PID function. Windup would continue to occur during periods where the PID was not active, resulting in unpredictable spikes in motor output when changing between tuning parameters or control modes. Integrator windup also exacerbated the consequences of the occasional noise over the serial connection. The resultant movements of the motor were sufficient to cause damage to the orthosis, and the PID.h library was eventually abandoned, and the motor controller written manually.

The rewritten controller was implemented with purely nonproportional integrator control. The controller output to the motor increases at a configurable constant rate up to a maximum when under the reference, and decreases at a different set rate when over the reference. Because the controller was coded manually, the windup value can be reset upon moving between different use-cases to avoid unpredictable motion. This controller replaced the imported PID controller during both the calibration procedure and Assist-As-Needed movements.

2.13 GUI

The graphical user interface (GUI) was constructed with Matlab's App Designer tool. It gives the user an interface through which to control the device, as well as displaying the current status of the device to the user. The default display was kept minimalist, as not to overwhelm the user, but they can navigate to an advanced display that includes additional data relevant to troubleshooting.

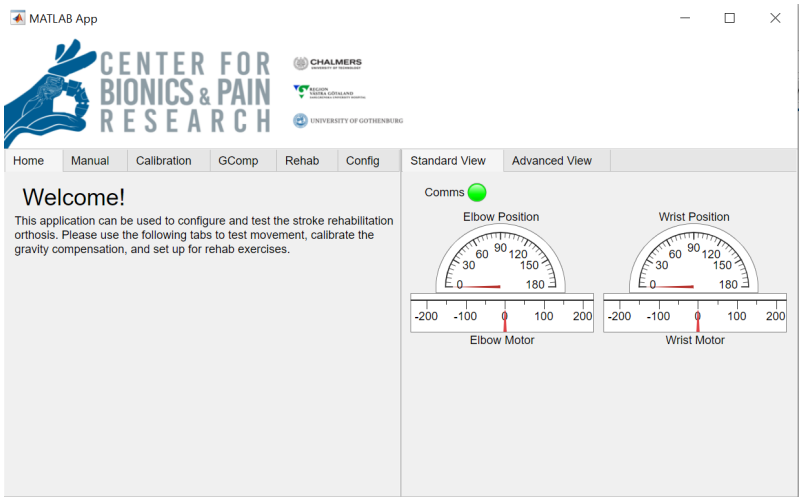

Figure 2.21: The home screen of the GUI. The right panel shows the status of the orthosis in intuitive and streamlined display.

The GUI has several tabs that allow for setup and testing of the orthosis. The 'manual' tab allows for testing of the elbow motor in position- or speed- based control. The 'calibration' tab allows the user to run the calibration sequence to generate a gravity compensation model. The 'gcomp' tab activates the current gravity compensation model without any other control present. The 'rehab' tab allows the user to trigger the assist-as-needed functionality in flexion and extension of the elbow and wrist joint. There is also the option to configure many relevant settings, such as reference position and velocity in different and controller tuning parameters in different modes.

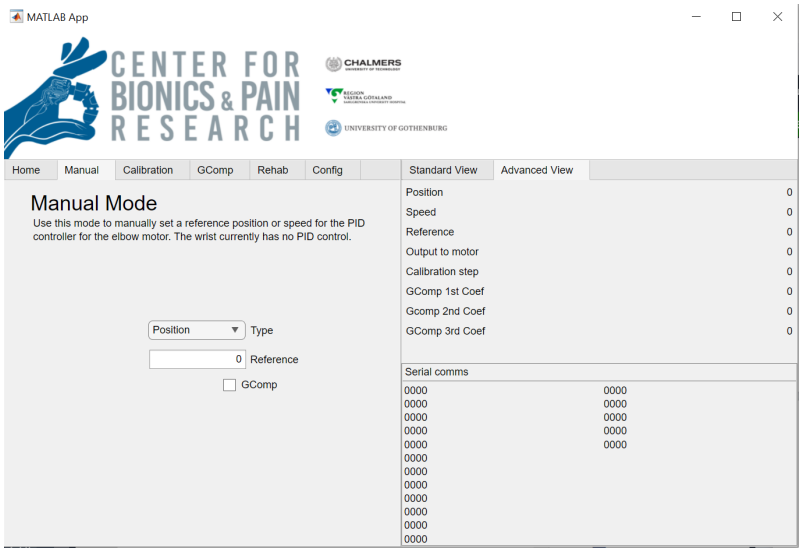

Figure 2.22: The GUI, open to the manual tab on the left and the advanced view on the right. On the manual tab the user can select between speed and position control modes, set a reference value, and optionally enable gravity compensation. The advanced view on the right shows the raw comms to and from the Arduino and gives important data as numeric values instead of visual representation.

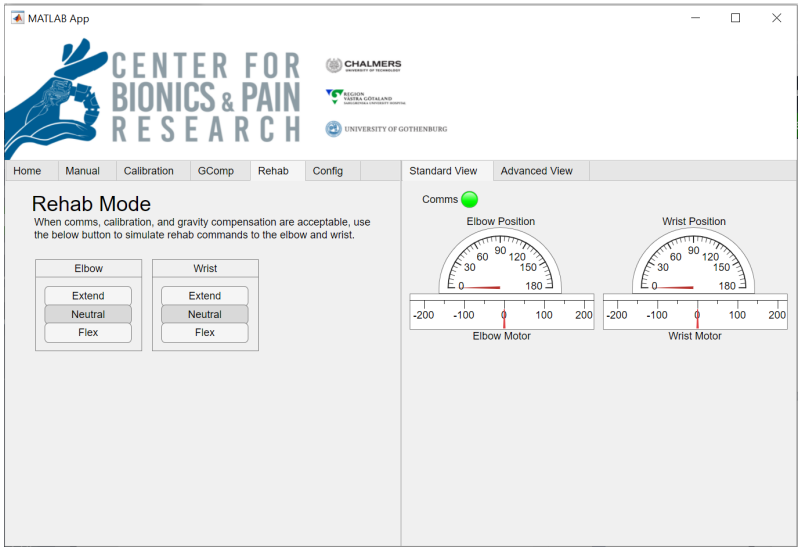

Figure 2.23: The GUI, open to the rehab mode. In this mode, the user can trigger flexion and extension movements of both joints, which activates the Assist-As-Needed functionality.

The GUI is a standalone app not incorporated into the BioPatRec system, therefore the rehab movements must be triggered manually through the buttons in the rehab tab instead of by reading the EMG signals in the arm muscles through BioPatRec.

3

Results

Several changes have been made to the orthosis to improve its functionality. Changes such as reducing backlash, and redesigning parts of the orthosis as well as the drivetrain. An active wrist function has also been added to now support wrist rehabilitation. The added complexity also led to circuitry, control scheme, and user interface changes. Many of the changes were inspired by other orthoses that the team at CBPR has access to. These were a great asset in giving potential ideas for improvements for the different problems the previous orthosis had.

3.1 Finished Orthosis

With all the aforementioned changes and improvements already implemented, the final iteration of the orthosis can be seen depicted in figure 3.1. It works as intended, with the required range of motion and intended functionality. All the electronics are stored in a compartment attached to the upper arm strut, and in figure 3.2, the orthosis can be seen worn by one of the group members from several views. The user can wear the orthosis without it obstructing the electrode placements, and it has a lot less play in it. The range of motion can be seen in figure 3.3, and it is comparable to the goal of 120°that was used during participant testing.

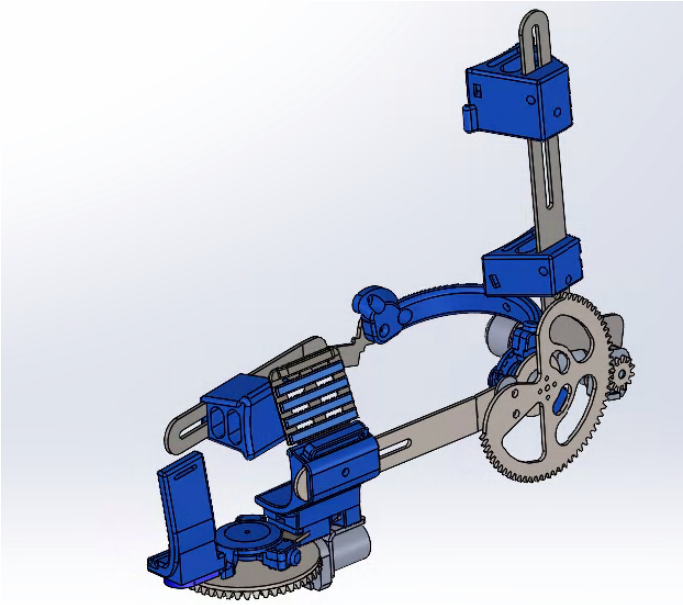

Figure 3.1: Finished orthosis seen in the CAD format, complete with both drive-trains, and it is adjustable depending on patient size

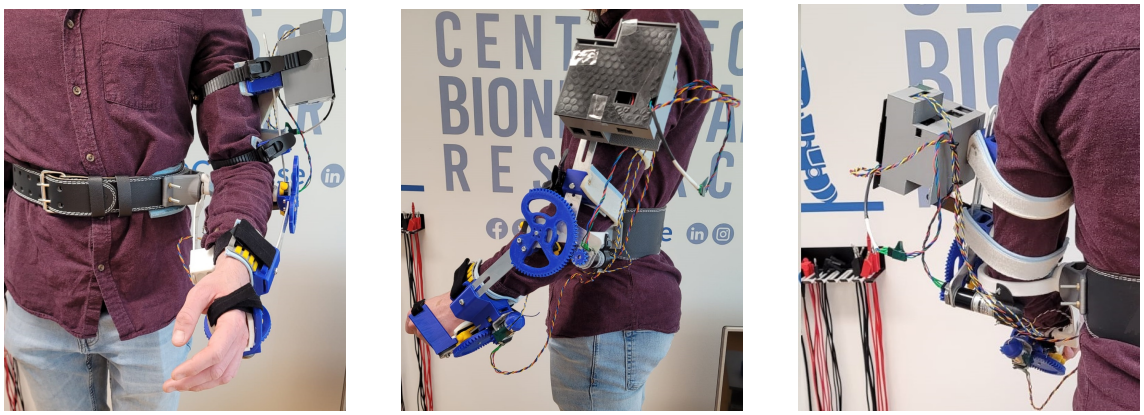

(a) Orthosis worn, ventral view

(b) Orthosis worn, lateral view

(c) Orthosis worn, dorsal view

Figure 3.2: Pictures of the orthosis worn by one of the thesis students from three different views.

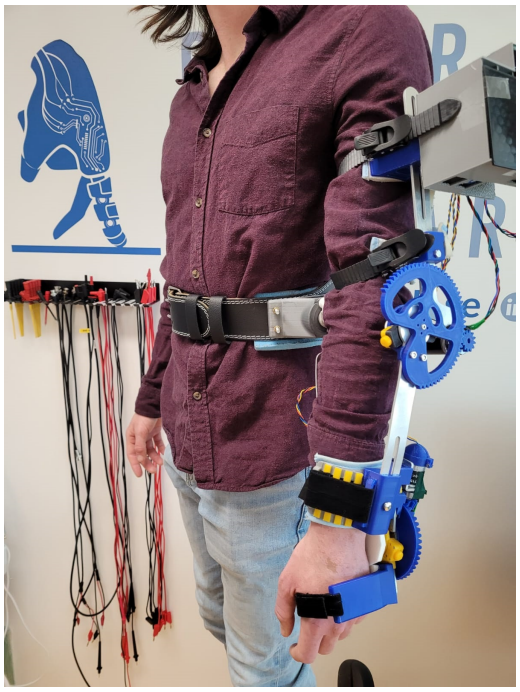

(a) Orthosis worn with full extension, approx 0°

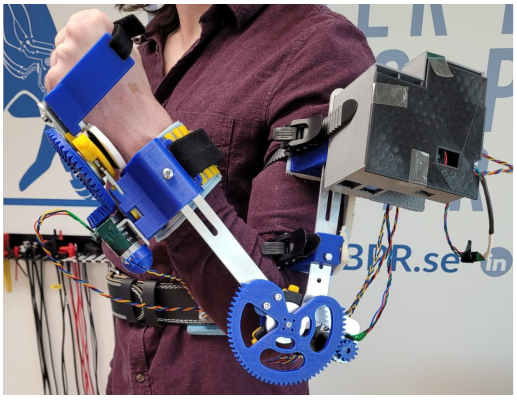

(b) Orthosis worn with full flexion, approx 150°

Figure 3.3: Range of motion of the orthosis while worn by one of the thesis students.

3.2 Exploring Calibration Models

To achieve gravity compensation, control was revamped from the position-based control of the previous system to torque-based output managed by programmatic control of the motor driving signal. With this control, an automated calibration sequence was developed that calculates a relationship between the current joint position and the motor input needed to compensate for gravity at that position. Early testing of the motor was conducted to confirm a second-order relationship can be observed between the position and motor input signal, then several different approaches were explored to find which resulted in the best model. The calibration sequence collects data to calculate the model by actuating the joint in PID mode and recording the motor torque (the driving signal from the controller) at specific locations. These preliminary tests to find a suitable calibration process with which to move forward were done with the orthosis attached to a test bench and weighted with a rubber simulacrum of an arm to approximate the correct rotational inertia.

The first version of the calibration sequence functioned by moving the elbow joint to 10, 50, and 90% of the total movement range via position-based PID control and taking data there. The gravity compensation model is calculated as a second-order polynomial from these three points, see figure 3.4.

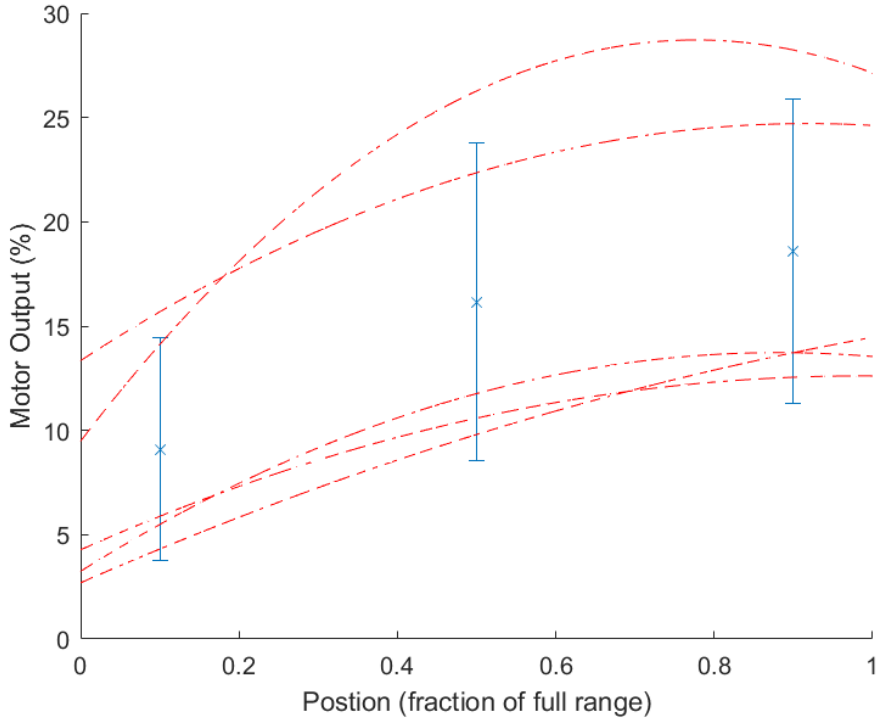

Figure 3.4: Data spread for five trials of the first calibration sequence. Blue bars represent the mean standard deviation of the sampled motor output at that location. Red lines represent the resultant polynomial fit for the five trials. Average standard deviation across all positions was 17.2.

There were quickly found to be forces within the system that were not well represented by the model, such as significant static friction, which creates a deadband of motor torque values for which the joint will not move. This caused the torque data collected at each data point to vary considerably between trials and resulted in a polynomial fit that poorly captured the gravity compensation needs. Preliminary qualitative assessments determined this approach was not worth pursuing further.

The second iteration of the calibration sequence attempted to account for the movement deadband caused by static friction in the system. In this version, the joint actuates in speed-based PID control to slowly and steadily sweep across the whole range of motion between the two hard stops, collecting data at 10, 30, 50, 70, and 90% of the range. Then, the sweep is repeated in reverse, capturing the motor input at the same positions while moving in the negative direction. All 10 data are used to estimate a line of best fit. This is done via a least-squares regression to produce a second-order polynomial using the Arduino curveFitting library [45].

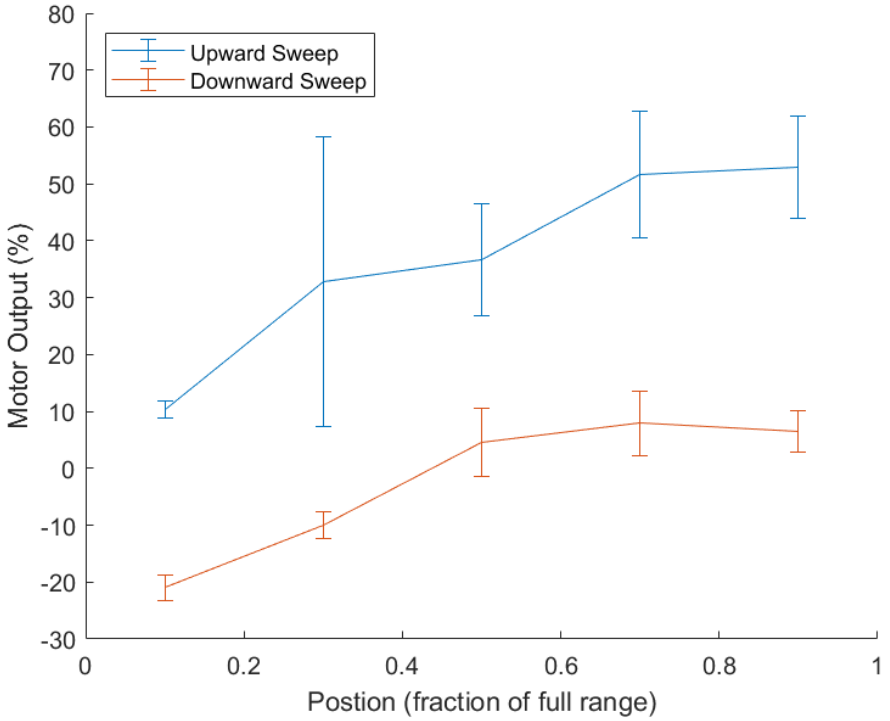

Figure 3.5: Data spread for five trials of the second iteration of the calibration sequence. For this sequence, motor output data was collected at five evenly spread points along the range of motion. Line represents mean of five trials with error bars representing standard deviation. Average standard deviation across all positions and directions was 19.6.

This sequence proved superior to the first sequence in repeatability but still had shortcomings. The control would still occasionally overshoot the target, sometimes by enough to require the calibration process to be restarted. Also, the extremes of the range of motion were found to be pushing too hard – the model applied too much negative torque when approaching the negative hardstop and too much positive torque near the positive hardstop, creating "suction points" toward the hardstops that were difficult to move away from. Again, this approach was discarded, and the calibration process was iterated.

In the third version of the calibration sequence, the data collection is expanded to be nine different points in each direction for a total of 18 data, happening at 10, 20, 30, 40, 50, 60, 70, 80, and 90% of the movement range while the joint actuates, again in speed-based control. Each pair of positive-sweep and negative-sweep samples are averaged together, and the final nine data points are used as a piecewise function to determine the ideal motor torque at each location. It was also before the implementation of this third sequence that the imported PID controller was rewritten into the nonproportional integral controller as mentioned in section 2.12.

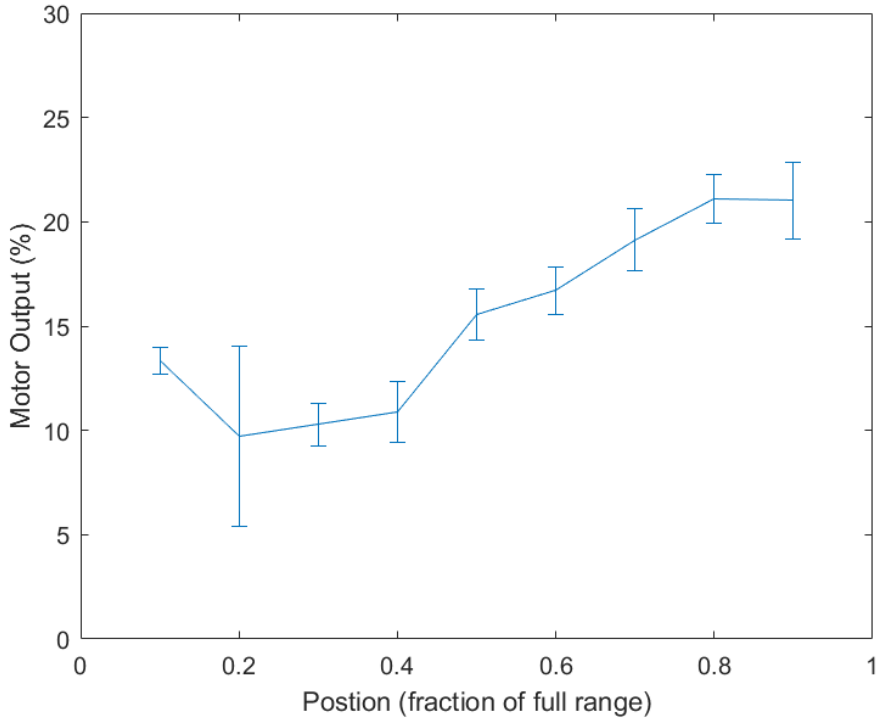

Figure 3.6: Data spread for five trials of the third iteration of the calibration sequence. For this sequence, gravity compensation at each point is the average of the motor output when sweeping up and down through that point. Line represents average of five trials, with error bars representing standard deviation. Average standard deviation across all positions was 4.0.

This third calibration sequence improved on the issues with the previous two, and was deemed worthwhile to pursue with further testing. A 'default' calibration was also developed, where the output values for each step of the model were hand-chosen based on the data observed during calibrations. These were set at [0, 7.8, 11.8, 15.8, 17.6, 19.6, 19.6, 17.6, 15.6] as percents of motor output.

3.3 Preclinical Trials

When testing the orthosis, the safety and comfort of the participant always come first. The orthosis was not cleared to be worn until safety measures had been verified: emergency disconnects to stop unwanted motor movement, hard stops to prevent over-extension of the joints, and programmed backup measures to prevent garbage data in the serial communications from causing erratic behavior of the motor. Before testing the orthosis on participants, several tests were made to ensure that the orthosis would not malfunction during use. When the orthosis was deemed safe for human use, it was donned by one of the master's thesis group members. After that, a pilot study was conducted, and from that, testing on other healthy participants was conducted. The participants were all healthy university

students. Seven trials were conducted, during three of which were experienced unrecoverable mechanical/electrical issues that required stopping the trial before completion. Incomplete data from the unsuccessful trials was thrown out, resulting in a study size of 4 for the trial results presented.

During each session, the participants had a set of questions to evaluate the orthosis based on different criteria. There were also some tests in place to compare the baseline calibration to the personalized calibration. These calibrations are evaluated at different angles to see how the gravity compensation model acts at these points since gravity differs depending on the angle, see figure 3.7. There was also an open field after most questions where the participants were asked to elaborate further on their grades. These scores are collected and presented in the following tables 3.1.

Table 3.1: Table of the results from the orthosis evaluation, presented as the mean score as well as the standard deviation of said score. 1 being difficult/unsafe and 5 being easy/safe.

	Mean	Standard deviation
How did you perceive the ease of donning the orthosis? (1-5)	4	0
How intuitive was the ratcheting device to use? (1-5)	4.25	1.5
How did you perceive the comfort during the calibration of the orthosis? (1-5)	3.5	1.73
Did you feel safe while wearing the orthosis during AAN elbow flexion/extension? (1-5)	4.25	0.96
Did you feel safe while wearing the orthosis during AAN wrist flexion/extension? (1-5)	5	0
How do you perceive the ease of doffing the orthosis? (1-5)	4	0.82

There were significant hardware issues while attempting to collect participant data during the trials. The first trial was called off due to the elbow encoder malfunction. This was diagnosed as being due to lateral force on the encoder rings from the motor shaft. The motor cap was realigned to center the motor to remove the lateral force, and this sustained the orthosis through the second trial. In the third trial, progressive warping of the metal strut caused the elbow gear alignment to become so poor that the gears would frequently skip while attempting to move. This skipping invalidated the encoder position feedback used in the controller. This was problematic enough to necessitate canceling the third trial. A new elbow motor cap was printed, and the pinion gear was replaced with a less worn backup. This lasted through one more successful trial, before the metal strut got misaligned again, which repeatedly needed bending back into place after each trial. After learning about this and the

previously mentioned changes, the remaining two trials proceeded with only minor recoverable issues.

3.4 Gravity Compensation

Another part of the test involved user evaluation of the gravity compensation. This evaluation was performed once using the gravity compensation model generated by the calibration sequence, and once using the default model. The participant was asked to move their arm to specific angles and report how they perceived the gravity compensation. The results of this test are shown in figure 3.7.

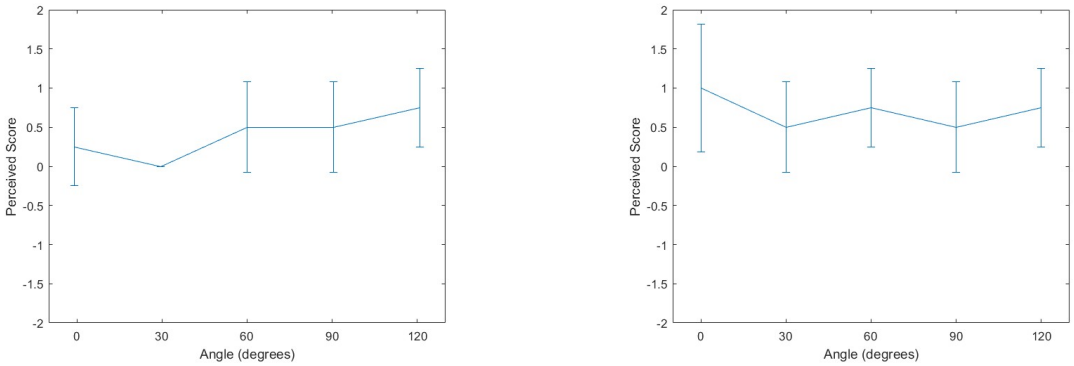

Figure 3.7: Errorbar comparing the default (left) and calibrated (right) gravity compensation models based on participant feedback. Scoring is based on these points of evaluation, where 0 is ideal: Moved down on its own = -2, Pushed down = -1, Well balanced = 0, Pushed up = 1, Moved up on its own = 2.

Both of these calibrations proved comparable with a mild bias towards the positive direction, with the majority of responses as either 'well balanced' or 'pushed up'.

Open field responses during this section repeatedly called out the sudden shift in motor output as it moved between discrete steps, specifically for the default model, where moving between the first and second steps causes the motor output to jump by 20 units. Participants were also asked if they perceived any delay in the responsiveness of the gravity compensation model, to which all four participants answered 'no'.

3.5 Assist-As-Needed

To evaluate the Assist-As-Needed functionality, participants were asked to perform three flexion-extension cycles for both the elbow and the wrist separately, in time with the assist functionality being triggered via the GUI. All participants were able-bodied and were instructed to only use the minimum force necessary in an attempt to approximate the experience of a stroke patient. The default gravity compensation

was active during this exercise, with the gravity compensation component and the Assist-As-Needed component being combined to create the motor input. The results of this part of the trials are shown in table 3.2.

Table 3.2: Summarised results regarding assistance as needed, scale going from 1-7, 1 being *gave no assistance* and 7 being *moved the arm by itself*. Ideally, the response should be just enough assistance to aid in the movement without doing the work for them, so a score of 4.

	Mean	Standard deviation
How much did the assist functionality aid in elbow flexion/extension? (1-7)	3.5	1
How much did the assist functionality aid in wrist flexion/extension? (1-7)	3.25	0.96

Open field responses for the elbow assist evaluation repeatedly mention the flexion being easier than the extension. Other comments mentioned how the movements felt smoother when the participant moved slowly.

During the trials, the wiring to the motor driver was malfunctioning which caused the wrist to not be able to apply any assistance in the extension direction. This was not explained to the participants nor was it visible through the GUI. The open field responses during the wrist assist evaluation were split, with two participants mentioning not being able to feel the assistance at times. More comments mentioned that the wrist assistance was very weak, which made it difficult to discern when it was present or not.

4

Discussion

We ran a total of seven tests, of which four were successful, and three could not be completed. The tests evaluated the effectiveness of the orthosis as a prototype for a stroke rehabilitation device.

4.1 Mechanical Performance

One of the biggest challenges with the prototype was the gear alignment. The bearings used had some inherent issues, such as the tapped hole in the bearing being off-centered, which made the gear rotate irregularly. This issue was, however, overshadowed by another flaw in the system. Due to the low strength of the struts, if not supported correctly, different externally applied forces can bend the metal. Thus misaligning the gears, see figure 4.1 for a view of how one of the struts got bent while in the test rig. The issue would best be fixed with new struts made of a better material to provide stability and prevent unintended flexion. This is also a trade off where weight and price needs to be kept low without compromising too much on the mechanical structure. This need for new struts would be a great opportunity to see if anything that could potentially fit the criterion was available on the market today, as this would remove the need for custom-made parts and hopefully bring down costs.

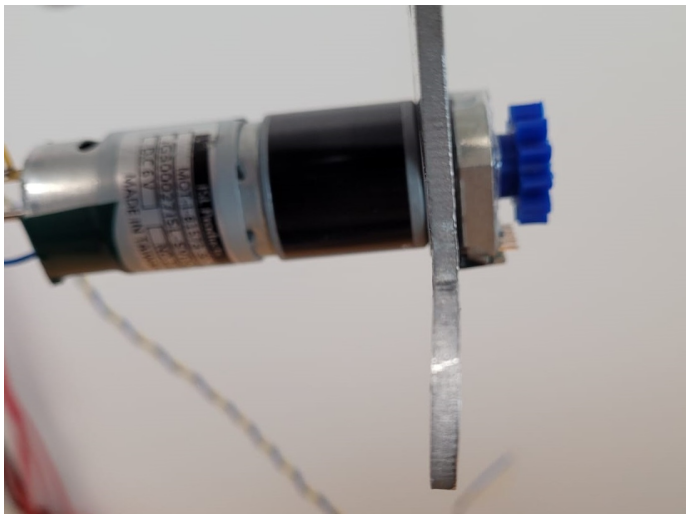

Figure 4.1: Picture of how the aluminum strut got bent from external forces during testing with the test rig.

Most components on the orthosis are 3D printed, such as the sliders, and are therefore more available to the general population as it does not involve precision metal cutting. The final iteration of the orthosis uses 3D-printed gear since those were easier to manufacture in-house than metal gears. The PLA gears tended to wear down after a while, as seen with the metal gears used earlier during the project. An improvement would be to make these gears out of a stronger metal or buy gears available on the market with the desired gear ratio and size. This would extend the lifespan of these gears since the D-key of the hub tended to wear out quickly and render the gears useless.

4.2 Gravity Compensation

The two gravity compensation models that were tested both succeeded at holding the arm steady throughout the range. Given the movement deadband introduced by the friction in the joint, there was room for the motor to be unbalanced and still maintain the position of the arm. Both the calibrated model and the default model were within this range despite a positive bias. Notably, the deviation in responses for the calibrated model is not significantly smaller than the default model, which suggests that the variance between different users and scenarios is not presently a significant source of error to the performance of the gravity compensation compared to other factors, such as friction in the system. As all participants were able-bodied, so this may change for patients with variable degrees of motor impairment.

The positive bias in both models could come from a variety of sources. In the default model, this is likely due to the step values chosen, and different default values would potentially resolve the bias. However, while accuracy may be improvable, it is expected that there is an upwards limit to the precision with this model as user-nonspecific sources of error are diminished. In the calibrated model, this could result from the controller not being reactive enough to counter the momentum of the orthosis as it moves with gravity compared to against gravity.

Another theory to explain the positive bias in the calibrated model is the interaction between gear backlash and static friction. Gravity causes the gears to rest on the positive edge of the backlash, so they need to overcome static friction on both sides of the joint before moving. In the negative direction, there is a small amount of play, so the driving side experiences kinetic friction before needing to overcome the static friction of the driven side.

While the exact mechanism behind the bias is speculative, the presence of static friction as a large source of error is evident in the data. These frictional effects are difficult to account for, as the mechanical parts would warp and the gear alignment change even throughout the course of one trial. Techniques explored in the calibration procedure – such as averaging together an upward and downward sweep – approximate the center of the friction deadband, but there are other ways the data is complicated by these frictional effects. For example, the motor would initially be stationary and need to overcome the static friction to reach the second

sampling location. This often resulted in either significantly higher motor output in the second step or significantly lower as the joint began moving faster than the reference and coasted through the second location under momentum while the controller was attempting to slow it down. This can be seen in the large variability in motor output data for the second location in Figure 3.6 and the second step of the upward sweep in Figure 3.5.

Despite bias and frictional sources, the gravity compensation largely succeeded as the unbalanced forces were generally insufficient to move the arm when slack, meaning all movement would be from the users. It also improved the perceived delay in the system, which was a significant drawback of the previous orthosis design [3] and a big improvement in user-friendliness since perceiving delay in a system can be irritating and tedious.

4.3 Assist-As-Needed

The evaluation of success in providing Assist-As-Needed functionality is difficult without an extended trial measuring the improvement over time of actual stroke patients performing rehabilitation exercises. Given that the current system does not integrate with BioPatRec and requires manual triggering of the flexion and extension movements through the GUI, the current system stands more as a proof of concept. Nevertheless, participant scoring for the assistance during these exercises indicates a favorable amount of aid without encouraging slacking for both the elbow and the wrist movements.

Often, the gravity compensation model worked against the assist functionality during elbow movements. Being able-bodied, most of the participants would not wait long enough for the assist function to build considerably before moving the joint under their own power, so the forces they experienced were largely dominated by the gravity compensation component and not the assist function. Since the gravity compensation models tended to push stronger in the positive direction, participants that did not wait sufficiently would feel the orthosis fight against them when trying to extend.

For the wrist movements, the participant scoring needs to be regarded with some dubiety as the wrist motor was not strong enough to provide adequate force during wrist flexion and, due to malfunction, was applying no force during extension. The forces calculated when choosing the wrist motor were based on calculations of moving a limp wrist, which was an oversight as the forces generated by an able-bodied person's muscles when flexing or extending the wrist joint are several times larger. The current motor was barely perceptible to the able-bodied participants and would not be able to oppose the spasticity of locking often present in the wrist joint of stroke patients, and a stronger motor is needed.

Compared to the previous orthosis, the implementation of the flexion and extension movements is a clear improvement and more in line with Assist-As-Needed function-

ality, as well as the addition of the wrist joint. Flexion movements were generally easier and smoother than extension movements, a trend that was also present in the previous orthosis despite the measurement parameters being different.

4.4 Serial Communications

The serial communications between the MATLAB GUI and the Arduino Nano proved to be a significant problem throughout the project. The Arduino serial communication is intended to send and receive individual bytes of data. While this was sufficient for the previous orthosis, the added functionality required communicating data larger or more precise than a byte allowed. A custom protocol was implemented to handle these communications between Arduino and MATLAB. The new protocol is the bare minimum necessary to communicate the needed data. It has several limitations, such as not handling negative numbers correctly, which were worked around to pass information back and forth successfully.

Additionally, the data through the connection periodically becomes jumbled, causing random bits to be passed mid-message. In the original orthosis, the communications were rudimentary to the point that the occasional garbage data was not noticeable. With the new communications, the GUI and the Nano were writing dozens of bytes back and forth every 100 ms. A momentary change in the PID reference during manual mode control potentially sends the motor at maximum power in either the positive or negative direction. Likewise, a momentary change in the control mode would cause similar erratic motor behavior or kick the user out of the calibration sequence mid-process and force them to restart indefinitely.

Exploration into the root cause of the communications disruptions pointed towards it arising from inherent issues in the nature of two-wire serial communications and not a product of the setup or due to a faulty cable or software installation. As such, garbage data can not be eliminated, only identified and dealt with. Further investigation into shielding to reduce noise and making more mechanically secure wiring may help reduce the occurance rate, but safeguarding sensitive processes from momentarily incorrect communications is still necessary.

Steps were taken to defend against these issues when identified. As much of the control was moved to the Arduino as possible so that the dependency on communicated data was minimized. A communications handshake was implemented, wherein the first message of every packet is a specific predetermined number that, when recognized by the other side, ensures the incoming message was not staggered. When garbage data is detected, it is purged until the start of the next message. Important incoming data that could cause erratic behavior if incorrect is held until several subsequent messages agree on the value before being committed to the runtime. Together, these efforts successfully nullified the consequences of incorrect data coming through the serial port and the 500 ms delay introduced was not detrimental to the perception of the GUI.

4.5 Towards Patient Trials

At the end of this project, the orthosis is still in the prototype stage and is able to demonstrate functionality in the small study of able-bodied participants. Still, it requires further development before being extended to tests on actual stroke patients.

The Orthosis would need to be integrated into the BioPatRec (or MyoCognition) system so that the assist-as-needed function could be triggered by the EMG signal instead of directly through the GUI. The current GUI would need to be incorporated into the larger system, for example, being launched from a button within the system GUI. This poses some complications, as the serial communications of the orthosis GUI are significantly greater than the BioPatRec protocol, so a handoff would have to be developed that manages the transfer of the serial communications from the BioPatRec GUI to the orthosis GUI for the orthosis to be configured and calibrated, then transferred back for the actual rehab exercises.

The orthosis would also benefit from further development of the calibration model before advancing to patient trials. Less friction would improve the gravity compensation calibration model and allow personalized calibrated models to outperform the default model, and also open the door to more robust calibration strategies. The current model suffers from the user feeling the discrete steps as the compensation value jumps from one value to another. Running a low pass filter over the data to smooth out the discontinuities would likely improve the user experience without sacrificing the accuracy of the gravity compensation.

From the test that were conducted, there were several improvements pointed out by the participants. For one, the lower bicep ratcheting strap was a point of discomfort for all patients. This limited the range of motion, and visible irritation in the skin was seen after the test was conducted. The test lasted between 20-40 minutes, and the hypothetical one-hour rehabilitation session would only exacerbate this issue. Other comments mentioned the fact that the attachment angle was hard to achieve while donning since the arm was in the way of getting that angle. This could be solved by changing the steepness of the sliders, allowing the ratcheting devices to attach at a more accessible angle. Furthermore, the straps hang loose and were hard to reach with the right arm, making donning more difficult. These factors added some complexity while donning and doffing the orthosis, which despite this, got a good grade from the participants.

It is worth noting that during the donning and doffing of the orthosis, the participants were asked only to use their right arm. This was an attempt to depict an unable-bodied patient using the orthosis more accurately. There were instructions on how to don and doff the orthosis that each participant followed, and extra verbal assistance was given when asked for. This mainly applied to the ratcheting devices since those could lead to confusion if never used before. The ratcheting devices were well received by the participants despite being less intuitive than normal velcro

straps.

There was also feedback regarding the waist-belt, which got complaints about being unreliable and unsuitable for bigger patients since the circumference was small. A bigger belt could be bought in the future to accommodate larger patients since the belt bought was intended for a specific patient in mind by the previous group. Suggestions to add a shoulder support from the right shoulder were made since some patients perceived that the orthosis tended to limit blood flow in the upper arm when tightened. The feedback suggests that the play has been reduced and the orthosis sits well on the user. However, it is difficult to evaluate how much better it fits since there are no previous assessments of comfort to compare it with.

Some concerns regarding over-extension of the elbow were brought up during the calibration sequence. This can be seen in table 3.1 where this category scored the worst and had the biggest standard deviation. This was due to the fact that in order to find the endpoints of the range of motion, the motor keeps pushing until it exceeds a predetermined torque value, and due to the placement of the hardstop, this was only achieved at fully extended elbows. The motor strength was insufficient to pose any danger to able-bodied participants, though mild discomfort was possible in the case of hardware failure.

5
Conclusion

Before any further testing on stroke patients is conducted, these aforementioned improvements should be implemented. The orthosis is safe for healthy participants, but the time did not allow patients to try it. It is the unfortunate reality of being unable to get feedback from these patients, as they are the primary user and insights into how they perceive the orthosis would be useful for further development. It is hoped that the development of this orthosis continues in future master's thesis projects so these improvements can be implemented and tests performed to get a proper evaluation of the orthosis function with its intended users.

The orthosis works as a proof of concept for a rehabilitation tool but due to not testing on actual patients no concrete conclusions can be drawn. However, when looking over the responses from the healthy participants, the results are promising, and with a few improvements, the orthosis should be ready for some patient testing.

5.1 Goals and criterion

In general, the orthosis largely achieves the objectives set forth by the project for the case of able-bodied participants, but with clear room for further improvement. Evaluation of the effectiveness of these solutions depends on doing a further study with stroke patients and benchmarked tests, and there are significant steps that need to be taken before the orthosis is ready for such trials. When evaluating the four goals set up for the thesis, the breakdown is as follows:

1. *Implement gravity compensation and assist-as-needed functionality into the elbow actuation.*

   The orthosis now has gravity compensation and assist-as-needed functionality. The gravity compensation is sufficient to support the arm against the force of gravity along the entire range of motion and reacts without delay, and with the overcoming of some hardware shortcomings there can be further development of better balanced models. The assist-as-needed function shows promise in striking a balance between aiding the user without promoting slacking, but would need testing with actual stroke patients for conclusive feedback, which would require integrating the orthosis into the BioPatRec or MyoCognition platforms.

2. *Implement some means for the device to be worn while training the EMG classifier so that the BioPatRec model translates well to rehabilitation exercises.*

   The back-drivability function was added with the new DC motor, which allows the orthosis to be worn while training the EMG classifier. The bicep and triceps are left uncovered by the orthosis attachments to allow for electrode placement, and the new electrical box has space for the BioPatRec system. However, software development never reached the point of integrating the orthosis with BioPatRec, so this system was never tested.

3. *Improve upon the physical design of the orthosis by reducing play, increasing comfort, and making it easier to don with one hand.*

   We believe the physical design has reduced play, but the upper arm metal strut is definitively not up to par with the quality we want for the final product. The press-fit bearing is poorly connected, and the strut is easily bent, leading to many complications. The mechanical comfort is largely the same, but the perceived comfort of wearing the orthosis while moving was improved. Furthermore, it might not be easier to don due to the added complexity of the ratcheting devices, but the perception was still positive. Future patient studies are needed to evaluate on the user group, but from the preliminary studies, the results are promising.

4. *Investigate adding a second degree of freedom in wrist flexion and extension.*

   A wrist flexion/extension DOF was added and evaluated. Despite some of the motor being slightly weaker than needed, it will still be seen as an improvement compared to having nothing. Further development would improve the effectiveness vastly and patient testing is needed to evaluate the functionality.

6
Work Contribution

The division of writing on this thesis largely follows the division of labor within the project. Sections addressing the hardware and mechanical design are written by Christoffer, and sections about the electrical, programming, and control are written by Kyle. The introduction is adapted from the initial literature review and follows the same work division as discussed therein. Sections that come together to discuss the project as a whole were worked on jointly.

Bibliography

[1] Hummel F. C Raffin E. "Restoring motor functions after stroke: multiple approaches and opportunities". In: (2018). DOI: 10.1177/1073858417737486.

[2] Joel Stein et al. "Electromyography-controlled exoskeletal upper-limb–powered orthosis for exercise training after stroke". In: *American journal of physical medicine & rehabilitation* 86.4 (2007), pp. 255–261. URL: https://journals.lww.com/ajpmr/Fulltext/2007/04000/Electromyography_Controlled_Exoskeletal.00002.aspx.

[3] Ragnhild Kilborn and Rebecka Lövgren. "Design of an active orthosis for improved rehabilitation of stroke patients". In: *Department of Biomedical Engineering, LTH* (2022). URL: https://lup.lub.lu.se/student-papers/search/publication/9089836.

[4] American Strokre Association. *About Stroke*. 2023. URL: https://www.stroke.org/en/about-stroke (visited on 01/31/2023).

[5] Angus J. C. McMorland, Keith D. Runnalls, and Winston D. Byblow. "A Neuroanatomical Framework for Upper Limb Synergies after Stroke". In: *Frontiers in Human Neuroscience* 9 (2015). ISSN: 1662-5161. DOI: 10.3389/fnhum.2015.00082. URL: https://www.frontiersin.org/articles/10.3389/fnhum.2015.00082.

[6] et al. Juan C. Cortes MD. "A Short and Distinct Time Window for Recovery of Arm Motor Control Early After Stroke Revealed With a Global Measure of Trajectory Kinematics". In: *Neurorehabilitation and Neural Repair* 31 (2017). DOI: 10.1177/1545968317697034. URL: https://journals.sagepub.com/doi/pdf/10.1177/1545968317697034.

[7] Flint Rehab. *How to Overcome Synergistic Movement After Stroke (When One Movement Leads to Many)*. 2022. URL: https://www.flintrehab.com/synergistic-movement-stroke/ (visited on 01/30/2023).

[8] Henry Hoffman. *The Brunnstrom Stages of Stroke Recovery*. 2018. URL: https://www.saebo.com/blog/the-stages-of-stroke-recovery/ (visited on 01/31/2023).

[9] et al. Thijs Krabben. "Influence of gravity compensation training on synergistic movement patterns of the upper extremity after stroke, a pilot study". In: *Journal of NeuroEngineering and Rehabilitation* 9.44 (2012). URL: https://doi.org/10.1186/1743-0003-9-44.

[10] David J Gladstone, Cynthia J Danells, and Sandra E Black. "The Fugl-Meyer assessment of motor recovery after stroke: a critical review of its measurement properties". In: *Neurorehabilitation and neural repair* 16.3 (2002), pp. 232–240. URL: https://pubmed.ncbi.nlm.nih.gov/12234086/.

[11] Nuray Yozbatiran, Lucy Der-Yeghiaian, and Steven C Cramer. "A standardized approach to performing the action research arm test". In: *Neurorehabilitation and neural repair* 22.1 (2008), pp. 78–90.

[12] Gustavo Saposnik. "Virtual reality in stroke rehabilitation". In: *Ischemic stroke therapeutics*. Springer, 2016, pp. 225–233. URL: https://link.springer.com/chapter/10.1007/978-3-319-17750-2_22.

[13] Peter Langhorne, Julie Bernhardt, and Gert Kwakkel. "Stroke rehabilitation". In: *The Lancet* 377.9778 (2011), pp. 1693–1702. URL: https://www.sciencedirect.com/science/article/pii/S0140673611603255.

[14] Gustavo Saposnik, Mindy Levin, and Stroke Outcome Research Canada (SORCan) Working Group. "Virtual reality in stroke rehabilitation: a meta-analysis and implications for clinicians". In: *Stroke* 42.5 (2011), pp. 1380–1386. URL: https://www.ahajournals.org/doi/full/10.1161/STROKEAHA.110.605451.

[15] Bojan Milosevic, Simone Benatti, and Elisabetta Farella. "Design challenges for wearable EMG applications". In: *Design, Automation Test in Europe Conference Exhibition (DATE), 2017*. 2017, pp. 1432–1437. DOI: 10.23919/DATE.2017.7927217.

[16] Oluwarotimi Williams Samuel et al. "Intelligent EMG Pattern Recognition Control Method for Upper-Limb Multifunctional Prostheses: Advances, Current Challenges, and Future Prospects". In: *IEEE Access* 7 (2019), pp. 10150–10165. DOI: 10.1109/ACCESS.2019.2891350.

[17] Agamemnon Krasoulis, Sethu Vijayakumar, and Kianoush Nazarpour. "Multi-Grip Classification-Based Prosthesis Control With Two EMG-IMU Sensors". In: *IEEE Transactions on Neural Systems and Rehabilitation Engineering* 28.2 (2020), pp. 508–518. DOI: 10.1109/TNSRE.2019.2959243.

[18] Nawadita Parajuli et al. "Real-Time EMG Based Pattern Recognition Control for Hand Prostheses: A Review on Existing Methods, Challenges and Future Implementation". In: *Sensors* 19.20 (2019). ISSN: 1424-8220. DOI: 10.3390/s19204596. URL: https://www.mdpi.com/1424-8220/19/20/4596.

[19] Joel Stein et al. "Electromyography-controlled exoskeletal upper-limb–powered orthosis for exercise training after stroke". In: *American journal of physical medicine & rehabilitation* 86.4 (2007), pp. 255–261. URL: https://journals.lww.com/ajpmr/Fulltext/2007/04000/Electromyography_Controlled_Exoskeletal.00002.aspx?casa_token=kTN-BeSXIbYAAAAA:ny6xa8uUOj8q01XndajkiAXVJdnZ0SYwPmRwXpFrh468-lSgHIjLGF6xxL8yV63DkVdjOTbcg17cUxfNMuln1QVlucePdA.

[20] "Feasibility of an optimal EMG-driven adaptive impedance control applied to an active knee orthosis". In: *Robotics and Autonomous Systems* 112 (2019), pp. 98–108. ISSN: 0921-8890. DOI: https://doi.org/10.1016/j.robot.2018.11.011. URL: https://www.sciencedirect.com/science/article/pii/S0921889018304263.

[21] Edoardo Cantù et al. "Printed Multi-EMG Electrodes on the 3D Surface of an Orthosis for Rehabilitation: A Feasibility Study". In: *IEEE Sensors Journal* 21.13 (2021), pp. 14407–14417. DOI: 10.1109/JSEN.2021.3059308.

[22] Muhammad Zahak Jamal. "Signal Acquisition Using Surface EMG and Circuit Design Considerations for Robotic Prosthesis". In: *Computational Intelligence in Electromyography Analysis*. Ed. by Ganesh R. Naik. Rijeka: IntechOpen, 2012. Chap. 18. DOI: 10.5772/52556. URL: https://doi.org/10.5772/52556.

[23] University of Michigan Health. *Orthoses (Braces)*. 2022. URL: https://www.uofmhealth.org/conditions-treatments/rehabilitation/orthoses (visited on 04/20/2023).

[24] S. Simrock. "Control theory". In: *CERN Accelerator School: Specialized Course on Digital Signal Processing*. 2008.

[25] S. Moubarak et al. "Gravity compensation of an upper extremity exoskeleton". In: *2010 Annual International Conference of the IEEE Engineering in Medicine and Biology*. 2010, pp. 4489–4493. DOI: 10.1109/IEMBS.2010.5626036.

[26] Nahla Khraief Haddad2 Sana Bembli1 and Safya Belghith. "Adaptive sliding mode control with gravity compensation: Application to an upper-limb exoskeleton system". In: *5ième Congrès International Francophone de Mécanique Avancée (CIFMA 2018)*. Vol. 261. 06001. 2019. DOI: 10.1051/matecconf/201926106001.

[27] Parker W. Hill, Eric T. Wolbrecht, and Joel C. Perry. "Gravity Compensation of an Exoskeleton Joint Using Constant-Force Springs". In: *2019 IEEE 16th International Conference on Rehabilitation Robotics (ICORR)*. 2019, pp. 311–316. DOI: 10.1109/ICORR.2019.8779422.

[28] Leigang Zhang, Shuai Guo, and Qing Sun. "An Assist-as-Needed Controller for Passive, Assistant, Active, and Resistive Robot-Aided Rehabilitation Training of the Upper Extremity". In: *Applied Sciences* 11.1 (2021). ISSN: 2076-3417. DOI: 10.3390/app11010340. URL: https://www.mdpi.com/2076-3417/11/1/340.

[29] David J Reinkensmeyer et al. "Slacking by the human motor system: computational models and implications for robotic orthoses". In: *2009 Annual International Conference of the IEEE Engineering in Medicine and Biology Society*. Ieee. 2009, pp. 2129–2132. URL: https://ieeexplore.ieee.org/abstract/document/5333978?casa_token=3RWIbXjNeawAAAAA:2qEAGSwfB46qBbz-6Y6nCtgRRL1JIUB-LxBWyM1YPqovzCdlifSsfmNQzYKWtza7R_0Ywbg.

[30] Noemi Bitterman. "Design of medical devices—A home perspective". In: *European journal of internal medicine* 22.1 (2011), pp. 39–42. URL: https://www.sciencedirect.com/science/article/pii/S0953620510002001.

[31] Mikko Virmavirta Ahti Rahikainen. "Constant Power Model in Arm Rotation - A New Approach to Hill's Equation". In: *World Journal of Mechanics* 4.6 (2014). DOI: 10.4236/wjm.2014.46018. URL: www.scirp.org/journal/paperinformation.aspx?paperid=47446.

[32] John Challis and David Kerwin. "Quantification of the uncertainties in resultant joint moments computed in a dynamic activity". In: *Journal of sports sciences* 14 (July 1996), pp. 219–31. DOI: 10.1080/02640419608727706.

[33] Darren Sawicz. "Hobby Servo Fundamentals". In: (2012). URL: https://www.princeton.edu/~mae412/TEXT/NTRAK2002/292-302.pdf.

[34] Martin Tschiersky et al. “Gravity balancing flexure springs for an assistive elbow orthosis”. In: *IEEE Transactions on Medical Robotics and Bionics* 1.3 (2019), pp. 177–188. URL: https://ieeexplore.ieee.org/abstract/document/8770277.

[35] Markus Puchinger et al. “The retrainer light-weight arm exoskeleton: Effect of adjustable gravity compensation on muscle activations and forces”. In: *2018 7th IEEE International Conference on Biomedical Robotics and Biomechatronics (Biorob)*. IEEE. 2018, pp. 396–401. URL: https://ieeexplore.ieee.org/abstract/document/8487218?casa_token=0yphfIuQ-hYAAAAA:Z_3_0gjbmgEsbKZIRS9dmkgvZvGS_jvDWHtr8QoWIy2lyWqj9ITXuo_yhEXP3yVUgQal99VeJA.

[36] Fernanda Márcia Rodrigues Martins Ferreira et al. “Development of portable robotic orthosis and biomechanical validation in people with limited upper limb function after stroke”. In: *Robotica* 40.12 (2022), pp. 4238–4256. URL: https://www.cambridge.org/core/journals/robotica/article/development-of-portable-robotic-orthosis-and-biomechanical-validation-in-people-with-limited-upper-limb-function-after-stroke/52650751CBCC28AE5C1B4F43E0C1EEFB.

[37] Padmaraja Yedamale. “Brushless DC (BLDC) motor fundamentals”. In: *Microchip Technology Inc* 20.1 (2003), pp. 3–15. URL: http://electrathonoftampabay.org/www/Documents/Motors/Brushless%5C%20DC%5C%20(BLDC)%5C%20Motor%5C%20Fundamentals.pdf.

[38] Allan Joshua Veale and Shane Quan Xie. “Towards compliant and wearable robotic orthoses: A review of current and emerging actuator technologies”. In: *Medical engineering & physics* 38.4 (2016), pp. 317–325. DOI: https://doi.org/10.1016/j.medengphy.2016.01.010.

[39] URL: https://www.digikey.se/en/products/detail/isl-products-international/MOT-I-81573-30-27/17754387?s=N4IgTCBcDaILIHkAqBaAkigHARgKwHYBmFQgBhTHxAF0BfIA.

[40] URL: https://se.rs-online.com/web/p/dc-motors/2389715.

[41] Philipp Rostalski et al. “A hybrid approach to modelling, control and state estimation of mechanical systems with backlash”. In: *International Journal of Control* 80.11 (2007), pp. 1729–1740.

[42] URL: https://www.digikey.se/sv/products/detail/dfrobot/DFR0601/10279757.

[43] URL: https://www.digikey.se/en/products/detail/cui-devices/AMT103-2048-N4000-S/10468125.

[44] URL: https://www.arduino.cc/reference/en/language/functions/analog-io/analogwrite/.

[45] URL: https://github.com/Rotario/arduinoCurveFitting.

A

Appendix 1

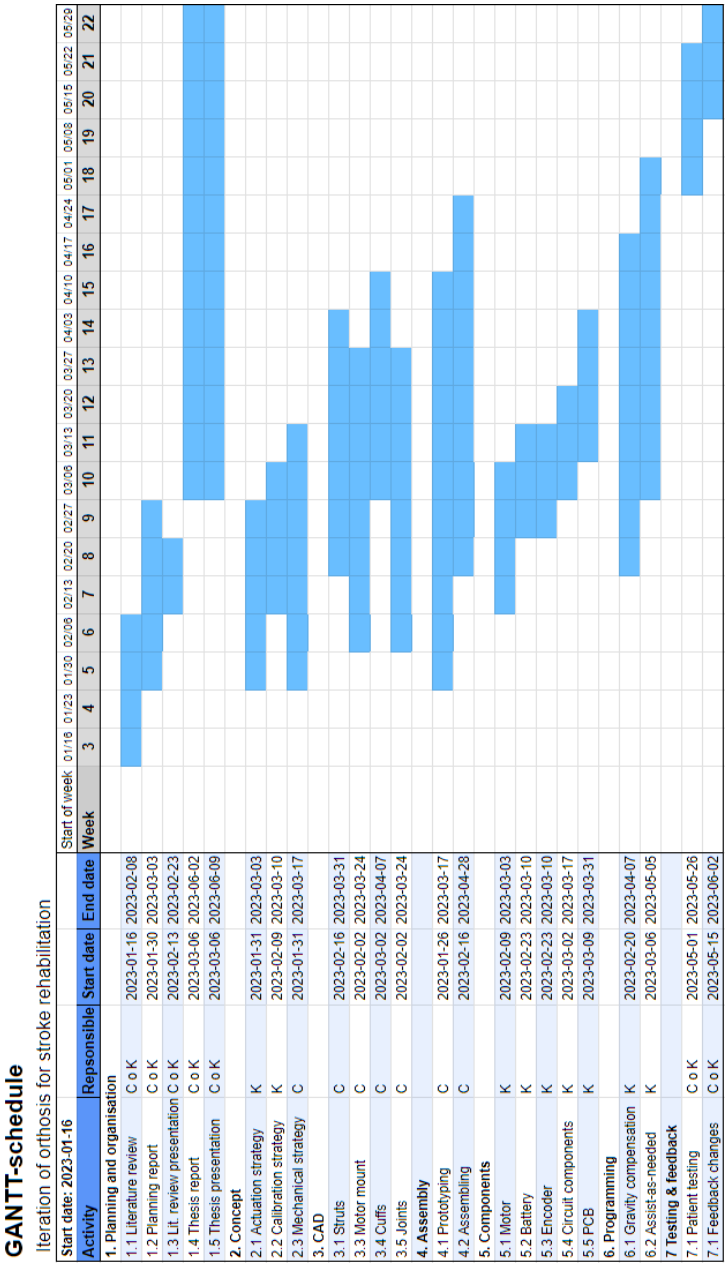

Figure A.1: GANTT schedule for the master's thesis plan.

DEPARTMENT OF ELECTRICAL ENGINEERING
CHALMERS UNIVERSITY OF TECHNOLOGY
Gothenburg, Sweden
www.chalmers.se

CHALMERS
UNIVERSITY OF TECHNOLOGY